Performance Analysis of TiO_2 Modified $Co/MgAl_2O_4$ Catalyst for Dry Reforming of Methane in a Fixed Bed Reactor

By

Arslan Mazhar

Reg # 00000277667

Session 2018-2020

Supervised by

Dr. Asif Hussain Khoja

A Thesis Submitted to US Pakistan Center for Advanced Studies in Energy in partial fulfillment of the requirements for the degree of MASTERS of SCIENCE in THERMAL ENERGY ENGINEERING

US Pakistan Center for Advanced Studies in Energy (USPCAS-E)

National University of Sciences and Technology (NUST)

H-12, Islamabad 44000, Pakistan

May 2021

Performance Analysis of TiO_2 Modified $Co/MgAl_2O_4$ Catalyst for Dry Reforming of Methane in a Fixed Bed Reactor

By

Arslan Mazhar

Reg # 00000277667

Session 2018-2020

Supervised by

Dr. Asif Hussain Khoja

A Thesis Submitted to US Pakistan Center for Advanced Studies in Energy in partial fulfillment of the requirements for the degree of MASTERS of SCIENCE in THERMAL ENERGY ENGINEERING

US Pakistan Center for Advanced Studies in Energy (USPCAS-E)

National University of Sciences and Technology (NUST)

H-12, Islamabad 44000, Pakistan

May 2021

THESIS ACCEPTANCE CERTIFICATE

Certified that final copy of MS/MPhil thesis written by Mr. Arslan Mazhar, (Registration No. 00000277667), of U.S.-Pakistan Center for Advanced Studies in Energy (USPCASE), NUST has been vetted by undersigned, found complete in all respects as per NUST Statues/Regulations, is in the allowable limits of plagiarism, errors, and mistakes and is accepted as partial fulfillment for award of MS/MPhil degree. It is further certified that necessary amendments as pointed out by GEC members of the scholar have also been incorporated in the said thesis.

Signature: _____

Name of Supervisor: _____

Date: _____

Signature (HoD TEE): _____

Date: _____

Signature (Principal/Dean): _____

Date: _____

Certificate

This is to certify that work in this thesis has been carried out by **Mr. Arslan Mazhar** and completed under my supervision in Fossil Fuels laboratory, USPCAS-E, National University of Sciences and Technology, H-12, Islamabad, Pakistan.

Supervisor: _____

Dr. Asif Hussain Khoja
U.S.-Pak Center for Advance Studies in Energy
NUST, Islamabad

GEC member 1: _____

Dr. Mustafa Anwar
U.S.-Pak Center for Advance Studies in Energy
NUST, Islamabad

GEC member 2: _____

Dr. Muhammad Hassan
U.S.-Pak Center for Advance Studies in Energy
NUST, Islamabad

GEC member 3: _____

Dr. Sehar Shakir
U.S.-Pak Center for Advance Studies in Energy
NUST, Islamabad

HoD-TEE: _____

Dr. Adeel Javed
U.S.-Pak Center for Advance Studies in Energy
NUST, Islamabad

Dean/Principal: _____

Dr. Adeel Waqas
U.S.-Pak Center for Advance Studies in Energy
NUST, Islamabad

Acknowledgements

All praise to Allah Almighty who gave me the strength and knowledge to do the work presented in this thesis.

I would like to express my sincere gratitude to my research supervisor Dr. Asif Hussain Khoja for letting me be part of the research group at Fossil Fuels Lab, USPCAS-E, NUST, Islamabad. I feel privileged to have worked under his kind supervision. It's the blend of his patience, determination, guidance and inspiration that made me accomplish my research aims in due time. He refined my research skills and I have learned a lot under his supervision and guidance.

I would also like to thank the members of my GEC committee, Dr. Mustafa Anwar, Dr. Muhammad Hassan and Dr. Sehar Shakir who honored my committee's presence. I would like to sincerely thank my fellows and specially, I pay gratitude to Lab Engineers Mr. Ali Abdullah, Mr. Asghar, Mr. Qamaruddin and Mr. Amir Satti for their unmatchable support during the whole research work.

Abstract

The synthesized Co/TiO_2-$MgAl_2O_4$ composite has been investigated for the Dry Reforming of Methane (DRM) process in the fixed bed reactor. The catalyst preparation was initiated by the modified co-precipitation method followed by hydrothermal method and the final nanocomposite was synthesized using impregnation method. The prepared catalyst undergone various characterization techniques such as X-ray diffraction (XRD), Scanning Electron Microscopy (SEM), Thermogravimetric analysis (TGA) and Fourier Transform Infrared Spectroscopy (FTIR). The catalyst was fed in the fixed bed reactor with the operational conditions of reactor temperature 850 °C, feed ratio (CO_2/CH_4) of unity, 0.5 g loading of catalyst and the total flow rate of feed set at 20 $mLmin^{-1}$. The product gases were analysed by gas chromatography thermal conductivity detector (TCD) analyser for the catalytic activity and stability results. For the various cobalt loading tests conducted, 5% Co loaded composite shown the higher catalytic performance with X_{CH4} and X_{CO2} of 70% and 80% while the selectivity results improved to 43% and 46.5% for H_2 and CO respectively. The average H_2/CO ratio of 0.9 was calculated for the overall operational time. Moreover the stability results indicated as much as 75 h time of stream with significant activity results showing 72% CH_4 conversion and 80% CO_2 conversion. The associated higher activity and stability results encourage the long run use of the catalyst in the DRM process along with the further modification and investigation need to be done in this aspect.

Keywords: Dry Reforming of Methane (DRM), TiO_2, $MgAl_2O_4$, Syngas, Hydrothermal process

Table of Contents

List of Figures

List of Tables

List of Abbreviations

Abbreviation:	Description:
GTL	Gas to liquid
FTS	Fischer Tropsch Synthesis
CCS	CO_2 capture and storage
GHGs	Greenhouse Gases
DRM	Dry reforming of Methane
POM	Partial Oxidation of Methane
SRM	Steam Reforming of Methane
TRM	Tri Reforming of Methane
XRD	X-ray Diffraction
SEM	Scanning Electron Microscopy
TGA	Thermogravimetric analysis
FTIR	Fourier Transform Infrared Spectroscopy
RWGS	Reverse water gas shift
MBSL	Multi-bubble sonoluminescence
ME	Micro emulsion
MFIBR	Magnetized fluidized bed reactor
HFMR	Hollow fiber membrane reactor
FBR	Fixed bed reactor
FIBR	Fluidized bed reactor
DCBR	Direct contact bubble reactor
TMR	Tubular membrane reactor
TCD	Thermal conductivity detector
NW	Nanowires
TOS	Time of stream

CHAPTER 1: INTRODUCTION

1.1 Research Background

The growing energy demands hang in balance with the increase in the world population and fossil fuels has led to meet the energy requirements over the years[1]. Greenhouse gases comprised of methane (CH_4), carbon dioxide (CO_2), nitrogen oxides (N_2O) and fluorinated gases. In recent years, keeping in mind the associated global warming effect, there has been rapid development in effective use of greenhouse gases emissions. Globally minds are shifted towards the energy storage and generation with the production of chemicals and the environmental issues kept in hand. The ultimate goal is to take benefit of the intense energy associated with the fossil fuel reserves being depleted and the production of clean and renewable fuels and chemicals[2]. Over the last 15 years, there has been access to the natural gas reserves which often contains CO_2 captured. Also many industrial processes result in the release of CO_2 into atmosphere leading to carbon capture and storage (CCS) technology in effect to reduce the emissions in environment[3].

Greenhouse gases (GHGs) production with methane and carbon dioxide being the major contributors having 16% and 76% exposure respectively to the environment has been the real issue to cope with the use of fossil fuels[4, 5]. Adding on to misery, CH_4 is 84 times more potent than CO_2 and has the major affect in global warming as it has 25 times global warming potential than that of CO_2[6]. The major sources of these gas emissions are industrial use, transportation and electricity production[7]. The GHGs emission sources, their contribution to global emissions and the pathway of major contributors of GHGs use has been shown in Fig 1.1.

Both CO_2 and CH_4 GHGs are cheap and available and the research is intended to be done with the focus on the activation of these gases with the production of liquid fuels and chemically valuable products[8]. Syngas (mixture of H_2 and CO) is the major intermediate of the industrial scale chemically conversion routes[7, 9]. Although

syngas can be generated using various routes but the catalytic reforming has gain much importance recently which include partial oxidation of methane (POM), steam reforming of methane (SRM) and dry reforming of methane (DRM) but the DRM process has advantage of using both GHGs as feed and production of syngas in unity proportion[10, 11]. So the DRM has clear environmental and economic benefits with syngas so produced can be further used for gas to liquids (GTL) applications.

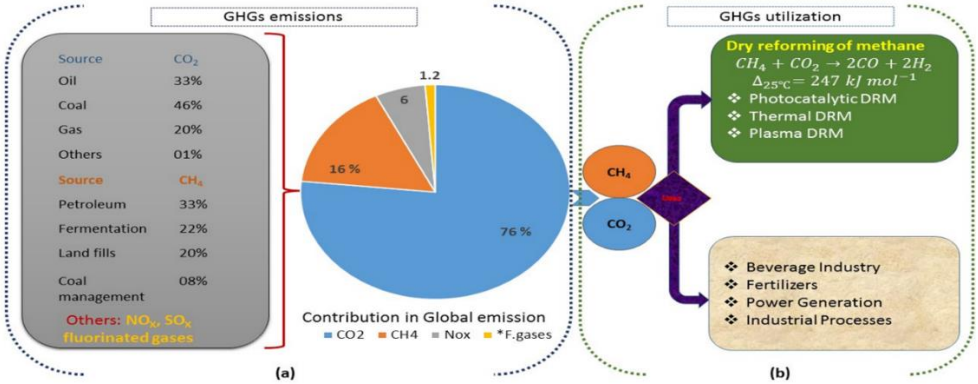

Fig 1.1 Sources of GHGs Emission and Utilization

With the environmental issues in line with the use of fossil fuels, the world is heading its way in need of the alternative resources and in search of that transition of solid to liquids and liquids to gaseous fuels has been implemented in the recent years as the source of energy[12, 13]. The renowned gas to liquid (GTL) technology is Fischer-Tropsch (FT) synthesis which is being practiced and it uses synthesis gas (syn-gas) which is fuel gas mixture comprising H_2 and CO_2 as a feedstock[14-20]. The typical gas to liquid process with FT synthesis is shown in Fig 1.2.

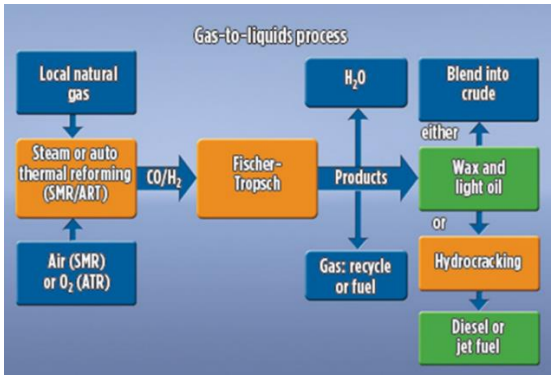

Fig 1.2 Gas to liquid (GTL) Technology[AK1] [21]

1.2 Problem Statement and Hypothesis

DRM has taken much attention because of the low installation cost, less energy consumption and the utilization of both GHGs for syngas and hydrocarbons production. Low conversions is still a major challenge in thermal DRM process due to carbon formation and deposition. The deposited carbon deactivates the active sites of catalyst, results in reactor blockage and lowering of DRM efficiency. Also catalyst stability is the major challenge in thermal DRM process. The use of catalyst with suitable metal-support combination can be effective to overcome and minimize the above mentioned effects.

The use of Co metal has the advantage of exhibiting better stability to carbon deposition. Additionally Co having high affinity for oxygen species will enhance the activity and stability. The use of support also effects activity and stability which depends upon the nature of support. For DRM process, for both CH_4 and CO_2 activation, the support with both acidic and basic properties is good and $MgAl_2O_4$ is an excellent support in this regard which provides strong metal-support interaction and high dispersion. Additionally $MgAl_2O_4$ shows good hydrothermal stability and mechanical strength. Bi-support can help in improving catalytic performance. Structured TiO_2 especially TiO_2 NWs is another excellent support which inhibit the carbon deposition and increase surface area assisting improvement in catalytic activity and stability.

1.3 Research Objectives

The focus of the work is to develop the catalyst having high stability and activity for DRM process and for that purpose following are the objectives of the research.

- To synthesize and characterize TiO_2 modified $Co/MgAl_2O_4$ catalyst for thermal DRM process.
- To investigate the catalytic activity of the modified $MgAl_2O_4$ catalyst in fixed bed thermal reactor.
- To investigate the stability of the modified $MgAl_2O_4$ catalyst in fixed bed thermal reactor.

1.4 Research Scope and Limitations

The research work followed three interacting phases which include catalyst synthesis and characterisations, activity tests and process optimization. In the first phase, catalyst was synthesized which included the supports synthesis from their precursors. The second phase comprises the composite formation from supports and metal combination followed by the characterisations named X-ray diffraction (XRD), Scanning electron microscopy (SEM), Thermogravimetric analysis (TGA) and Fourier Transform Infrared Spectroscopy (FTIR). The final phase included the activity and stability tests and process optimization of DRM in fixed bed reactor. This phase included various testing runs and various process conditions to get better catalytic performance results. The scope of work is shown in Fig 1.3.

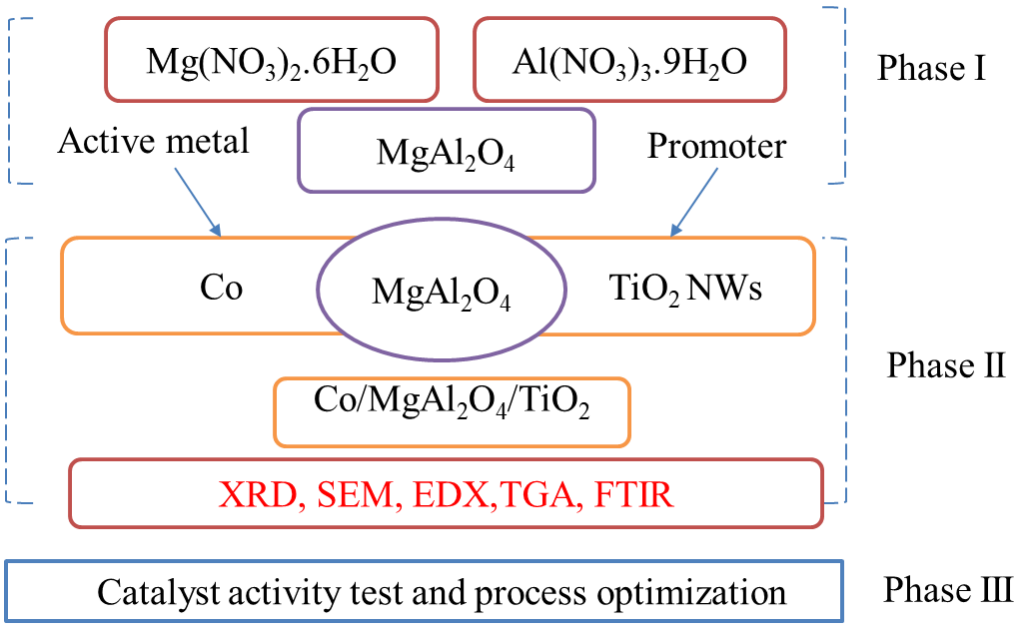

Fig 1.3 Research Scope Stages

The reactor design, upscale implementation of the work and DRM kinetics are some of the limitations that were beyond the scope of this research work. While the detailed present research work is written in methodology and results and discussion sections of this thesis.

Flow chart of Thesis

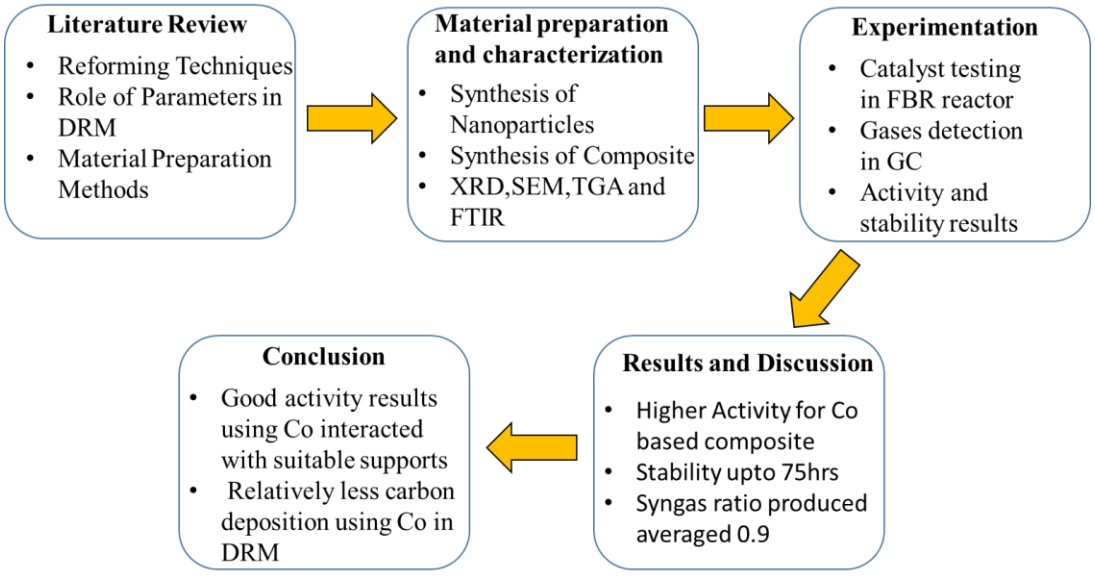

The literary review was initially done to find out the suitable metal and supports selection for DRM process and the effect of different parameters on the process. In the material preparation and characterisations section, catalyst was prepared and characterized. In the experimentation section, the prepared catalyst was undergone testing in reactor for activity and stability tests. In results and discussion section, detailed analysis of the results was discussed. Conclusive section dealt with the associated benefits of the catalyst used in DRM process and the application of the process on high scale keeping in mind the environmental friendly nature of the process

References

1. Li, X., *Diversification and localization of energy systems for sustainable development and energy security*. Energy policy, 2005. **33**(17): p. 2237-2243.
2. Er-Rbib, H., C. Bouallou, and F. Werkoff, *Dry reforming of methane–review of feasibility studies.* CHEMICAL ENGINEERING, 2012. **29**.
3. Bui, M., et al., *Carbon capture and storage (CCS): the way forward.* Energy & Environmental Science, 2018. **11**(5): p. 1062-1176.
4. Lashof, D.A. and D.R. Ahuja, *Relative contributions of greenhouse gas emissions to global warming.* Nature, 1990. **344**(6266): p. 529-531.
5. Lim, S.L., L.H. Lee, and T.Y. Wu, *Sustainability of using composting and vermicomposting technologies for organic solid waste biotransformation: recent overview, greenhouse gases emissions and economic analysis.* Journal of Cleaner Production, 2016. **111**: p. 262-278.
6. Boucher, O., et al., *The indirect global warming potential and global temperature change potential due to methane oxidation.* Environmental Research Letters, 2009. **4**(4): p. 044007.
7. Khoja, A.H., M. Tahir, and N.A.S. Amin, *Recent developments in non-thermal catalytic DBD plasma reactor for dry reforming of methane.* Energy conversion and management, 2019. **183**: p. 529-560.
8. Li, X., et al., *Greenhouse gas emissions, energy efficiency, and cost of synthetic fuel production using electrochemical CO_2 conversion and the Fischer–Tropsch process.* Energy & Fuels, 2016. **30**(7): p. 5980-5989.
9. Khoja, A.H., et al., *Thermal dry reforming of methane over La_2O_3 co-supported $Ni/MgAl_2O_4$ catalyst for hydrogen-rich syngas production.* RESEARCH ON CHEMICAL INTERMEDIATES, 2020.
10. Aziz, M., et al., *A review of heterogeneous catalysts for syngas production via dry reforming.* Journal of the Taiwan Institute of Chemical Engineers, 2019. **101**: p. 139-158.
11. Abdulrasheed, A., et al., *A review on catalyst development for dry reforming of methane to syngas: Recent advances.* Renewable and Sustainable Energy Reviews, 2019. **108**: p. 175-193.

12. Thomas, R.-N. and C. Today, *Manufacture of hydrogen.* Catal Today, 2005. **106**: p. 293-296.
13. Dunn, S., *Hydrogen futures: toward a sustainable energy system.* International journal of hydrogen energy, 2002. **27**(3): p. 235-264.
14. Delikonstantis, E., M. Scapinello, and G.D. Stefanidis, *Investigating the plasma-assisted and thermal catalytic dry methane reforming for syngas production: Process design, simulation and evaluation.* Energies, 2017. **10**(9): p. 1429.
15. Chen, G., et al., *Plasma-catalytic conversion of CO_2 and CO_2/H_2O in a surface-wave sustained microwave discharge.* Applied Catalysis B: Environmental, 2017. **214**: p. 114-125.
16. Karakaya, C. and R.J. Kee, *Progress in the direct catalytic conversion of methane to fuels and chemicals.* Progress in Energy and Combustion Science, 2016. **55**: p. 60-97.
17. Snoeckx, R., et al., *Plasma-based multi-reforming for Gas-To-Liquid: tuning the plasma chemistry towards methanol.* Scientific reports, 2018. **8**(1): p. 1-7.
18. Bromberg, L., et al., *Plasma reforming of methane.* Energy & fuels, 1998. **12**(1): p. 11-18.
19. Zhou, L., et al., *Nonequilibrium plasma reforming of greenhouse gases to synthesis gas.* Energy & fuels, 1998. **12**(6): p. 1191-1199.
20. Usman, M., W.W. Daud, and H.F. Abbas, *Dry reforming of methane: Influence of process parameters—A review.* Renewable and Sustainable Energy Reviews, 2015. **45**: p. 710-744.
21. Lipski, R., *Smaller-scale GTL enters the mainstream.* Gas Processing News. http://www. gasprocessingnews. com/features/201310/smaller-scale-gtl-enters-the-mainstream. aspx (Accessed on December 2018), 2012.

CHAPTER 2: LITERATURE REVIEW

2.1 Greenhouse Gases and Syngas

Greenhouse gases having more harmful impact on environment and abundancy seeks the proper capturing and storing of the gases and can be used in efficient processes producing high quality products like syngas.

2.1.1 CO_2 Capture and Storage

To reduce the amount of GHGs into the environment, several ways have been proposed to capture, store and utilize them in the effective way. Carbon capture and storage also known as CCS is one of them as this process includes the prevention of CO_2 release in large amounts in the atmosphere. The process includes the capture of CO_2 from the industrial plants and the fields of natural gas and after compressing it is then transferred into deep safe selected site rock formation for the permanent storage. The typical process of carbon capturing and storage is expressed in Fig 2.1.

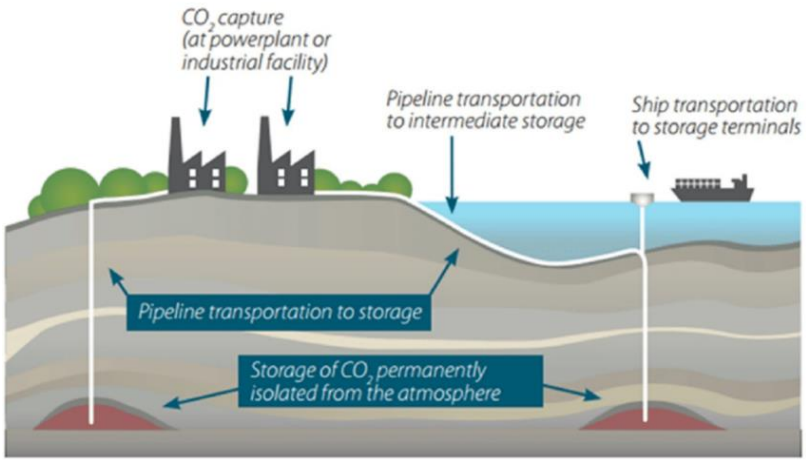

Fig 2.1 Carbon capture and storage principle

In Europe, similar demonstration of CO_2 capture and storage has been done by the introduction of Sleipner CCS plant which injects the pure CO_2 coming off the gas field into deep saline aquifer below sea and the estimation of the pure CO_2 coming off the field is over one million ton per year[1]. Similarly another source of CO_2 is Natuna D-Alpha gas filed which consists of 71% CO_2. Currently plans for the development of the 90% of CO_2 capturing and injecting it into deep beneath sea bed has been made[2].

Although CCS provides good option for the gas emissions reduction but it has certain limitations as well which include the capital investment in large amount, large storage needed for the gas storage and the consumption of large amount of energy. So the better option is that in addition to CO_2 storage, it must be further used for the chemical synthesis processes[3]. So instead of treating CO_2 as a waste it can be utilized for the reforming of CH_4 for syngas production as the thesis focus is also on this reforming technique of syngas production.

2.1.2 Syngas Importance

Syngas is the building block in the production of most of the chemicals and fuels including methanol, ethanol, FT oil and dimethyl ether (DME)[4, 5]. The major advantage of syngas is the inclusion of hydrogen as a component which itself is a clean fuel and can be obtained from various sources. Hydrogen finds its use in refineries, for example, processing of hydrogen and it has major applications in ammonia and methanol manufacturing. Syngas market is shown in Fig.2.2 with ammonia as the major contributor. The primary sources for the syngas production mainly includes coal, biomass and natural gas[6].

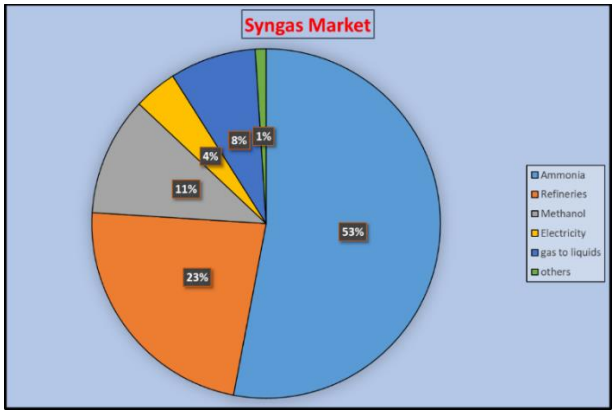

Fig 2.2 Present World's Syngas Market Contributors[7]

2.1.3 Reforming Techniques in Syngas Production

Using natural gas as a source, there are various methods to produce syngas but the reforming techniques has been the most attractive which use GHGs as a feedstock. The reforming techniques include steam reforming of methane (SRM), partial oxidation of methane (POM), dry reforming of methane (DRM) and tri-reforming of methane (TRM)[8, 9]. SRM has the higher syn-gas (H_2/CO) production in the molar ratio of 3:1 which is favourable for the hydrogen production but higher yield of hydrogen demands higher ratio of H_2/CO which may deactivate catalyst[10, 11].

For the FT synthesis and methanol production, SRM is unfavourable due to higher H_2/CO[12, 13]. SRM and DRM being endothermic require high energy input but for SRM, combustion of fossil fuel for energy input add on to the CO_2 emission but in case of DRM, CO_2 itself is used as primary constituent along with CH_4 for syngas production leading the reduction of emissions. POM although exothermic in nature finds operational difficulties and hot spot in catalysts and is suitable for the production of higher hydrocarbons[14].

DRM has the environmental advantage as it consumes both GHGs to process them for production of syngas reducing their concentrations in environment. Syngas (H_2/CO) is produced in the unity proportion in DRM which is favourable in FT synthesis in the production of higher hydrocarbons and oxygenated chemicals[15]

2.2 Overview of Reforming Technologies

The syngas mixture comprising of H_2 and CO is used for large scale production of many chemical products, fuels and mainly Fischer-Tropsch (FT) synthesis in gas to liquid (GTL) production[16, 17]. Although FT synthesis initiated with Dry Reforming of Methane (DRM) process but Steam Reforming of Methane (SRM) is the process which is being used for industrial scale production of syngas from natural gas. The disadvantages associated with SRM are higher syngas ratio which is not favourable for FT synthesis, highly endothermic reaction demanding higher energy input with high operational cost[1]. The other reforming technologies which include partial oxidation, autothermal reforming, dry reforming and tri reforming are the alternative routes for syngas production and the developments are being done in these areas.

The reforming processes are shown in the below equations:

Dry Reforming of Methane

$CH_4 + CO_2 \rightarrow 2CO + 2H_2$ $\Delta H°_{298K} = 247$ KJ/mol (1)

Steam Reforming of Methane (SRM)

$CH_4 + H_2O \rightarrow CO + 3H_2$ $\Delta H°_{298K} = 206$ KJ/mol (2)

Partial Oxidation of Methane (POM)

$CH_4 + 0.5O_2 \rightarrow CO + 2H_2$ $\Delta H°_{298K} = -32$ KJ/mol (3)

$CH_4 + 2O_2 \rightarrow CO_2 + 2H_2O$ $\Delta H°_{298K} = -802$ KJ/mol (4)

Auto thermal Reforming (ATR)

$CH_4 + CO_2 \rightarrow 2CO + 2H_2$ $\Delta H°_{298K} = 247$ KJ/mol (1)

$CH_4 + H_2O \rightarrow CO + 3H_2$ $\Delta H°_{298K} = 206$ KJ/mol (2)

Methane Cracking

$CH_4 \rightarrow C + 2H_2$ $\Delta H°_{298K} = 75$ KJ/mol (5)

As shown in the above equations, both DRM and SRM are endothermic reactions and require energy input but partial oxidation of methane (POM) is exothermic and don't require heat supply while the autothermal is self-sustaining type of reforming which has both exothermic and endothermic reactions. For POM, oxygen supply for reaction brings economic issues while SRM is used mostly for CH_4 reforming but it also requires steam production. The developments are being done in DRM process because it also utilizes CO_2 which is greenhouse gas.

2.2.1 Steam Reforming of Methane

Steam reforming reaction involves reaction between natural gas and steam which takes place in three steps namely reforming, shift and removal of CO_2 in conventional SMR process and is accompanied by the reactions given below.

$CH_4 + H_2O \rightarrow CO + 3H_2$ $\Delta H°_{298K} = 206$ KJ/mol (2)

$CH_4 + 2H_2O \rightarrow CO_2 + 4H_2$ $\Delta H°_{298K} = 163$ KJ/mol (6)

$CO + H_2O \rightarrow CO_2 + H_2$ $\Delta H°_{298K} = -41$ KJ/mol (7)

SRM uses eq.2 and eq.6 as reforming process in furnance to produce syngas where eq.6 leads to complete oxidation and resulting high production of hydrogen. Supplementary CH_4 is supplied to furnance as heat input owing to endothermic nature of steam reforming reaction. CO is reduced in the product to achieve the required syngas ratio by water gas shift reaction as shown in eq.7 while CO_2 is removed by adsorption technology[18]. Compared to other reforming processes, SRM is the most operational process on industrial scale in syngas and hydrogen production owing to being most economic and developed process.

2.2.2 Partial Oxidation

Partial oxidation of methane produces syngas ratio (H_2/CO) in 2:1 as shown in eq.3 but the indirect mechanism starts with the methane combustion as shown in eq.4 followed by DRM and SRM reactions to produce syngas[19].

$$CH_4 + 0.5O_2 \rightarrow CO + 2H_2 \qquad \Delta H°_{298K} = -32 \text{ KJ/mol} \quad (3)$$

$$CH_4 + 2O_2 \rightarrow CO_2 + 2H_2O \qquad \Delta H°_{298K} = -802 \text{ KJ/mol} \quad (4)$$

Partial oxidation of methane has some advantages over SRM as it is exothermic process and didn't require heat supply additionally it uses SRM and DRM reactions to make process more efficient. Also it produces syngas (H_2/CO) in the ratio 2:1 which is suitable for F-T synthesis. The pure oxygen supply and high pressure are the primary costs which make it economically impractical on industrial scale with additional costs of coke treatment and CO_2 separation.

2.2.3 Autothermal Reforming

Autothermal reforming is the combination of DRM, SRM and the oxidation process. This process use both endothermic and exothermic reactions hence leaving the heat input requirement to least possible by bringing balance of the heat from exothermic process and heat supply to endothermic process. Additionally this is more promising technique with better control in syngas production[20].

The process takes place in two zones: firstly the reaction of CH_4 with oxygen to produce CO_2 and H_2O and in the second zone the reaction of unconverted CH_4 with CO_2 and H_2O to produce syngas. The disadvantages linked with autothermal reforming

are the extensive control system for fuel processing system operation and sintering and deactivation of catalyst as a result of high temperature stream.

2.2.4 Dry Reforming of Methane

DRM is of significance importance because it uses both greenhouse gases (GHGs) and convert them into useful syngas. Syngas is produced in unity proportion as shown in eq.1. DRM reaction usually have three side reactions as shown in eq.5, eq.8, eq.9. Methane cracking is the decomposition of methane which usually occurs at low temperature resulting in carbon deposition which cause deactivation. Boudouard reaction is the decomposition of carbon monoxide into carbon dioxide and coke which occurs at high temperature and this reaction also causes deactivation[21].

Dry Reforming of Methane (DRM)

$$CH_4 + CO_2 \rightarrow 2CO + 2H_2 \qquad \Delta H°_{298K} = 247\ KJ/mol \qquad (1)$$

Methane Cracking

$$CH_4 \rightarrow C + 2H_2 \qquad \Delta H°_{298K} = 75\ KJ/mol \qquad (5)$$

Boudouard Reaction

$$2CO \rightarrow CO_2 + C \qquad \Delta H°_{298K} = -171\ KJ/mol \qquad (8)$$

Reverse Water Gas Shift

$$CO_2 + H_2 \rightarrow CO + H_2O \qquad \Delta H°_{298K} = 41\ KJ/mol \qquad (9)$$

Reverse Water gas shift (RWGS) reaction is another side reaction of DRM which affects the syngas ratio as more CO is produced with the reaction of hydrogen and carbon dioxide. Although DRM has certain advantages but its application on industrial scale is yet to be done.

2.2.5 Tri Reforming

Tri reforming is the synergetic combination of DRM, SRM and POM reactions in syngas production. This process has some unique advantages that combined DRM and SRM reactions help in achieving desirous syngas ratio and the major obstacle coming into DRM reaction was carbon formation. Integrating both SRM and POM with DRM resolve this issue by inhibiting the carbon formation[22].

2.3 Reaction Chemistry of DRM

DRM reaction is highly endothermic requiring high energy input which demands high temperature to carry out reaction producing syngas[23].

$$CH_4 + CO_2 \rightarrow 2CO + 2H_2 \quad \Delta H^{\circ}_{25^{\circ}C} = 247\ kJmol^{-1}\ (DRM) \qquad (1)$$

DRM additionally comes out with the simultaneous occurrence of reverse water shift gas (RWGS) reaction which results in the syngas ratio less than 1[24, 25].

$$CO_2 + H_2 \rightarrow CO + H_2O \quad \Delta H^{\circ}_{25^{\circ}C} = 41.0\ kJmol^{-1} \qquad (9)$$

The other major issue of DRM is the formation of the carbon which gets deposited as a result of side reactions which include methane decomposition and Boudouard reaction. Carbon formation on the surface of the catalyst occurs as a result of methane decomposition producing hydrogen.

$$CH_4 \rightarrow C + H_2 \quad \Delta H^{\circ}_{25^{\circ}C} = 75\ kJmol^{-1}\ (\text{Methane cracking}) \qquad (5)$$

The other way of carbon formation is the Boudouard reaction which shows the dissociation of CO into carbon and CO_2.

$$2CO \rightarrow C + CO_2 \quad \Delta H^{\circ}_{25^{\circ}C} = -172\ kJmol^{-1}\ (\text{Boudouard reaction}) \qquad (8)$$

DRM reaction proceeds at a temperature above 640 °C while the studies show the occurrence of side reactions at significant rate between 633 °C and 700 °C[26].Also the formation of water in reverse water gas shift reaction is up to temperature of 820 °C. So the high temperature is required to carry out the DRM reaction inhibiting side reactions but the excess temperature results in the blockage of the reactors due to the carbon deposition and activity reduction[27, 28].

DRM process need to be performed at a temperature less than 700 °C from the economic and technical point of view but it requires stable and active catalysts to be used in the process which inhibits carbon formation shifting reaction towards DRM. Previous studies show that among the catalysts, Ni and Co come out to be more effective. Moreover addition of Al_2O_3 results in the increased activity of the catalyst[29]. Different species of carbon form at different temperatures which play different roles in the DRM process. Ni/Al_2O_3 exhibited three different carbonaceous species named α-C, β-C and γ-C that formed during the reaction. It was observed that α-C aided in the formation of CO and also α-C increased with the proceeding of the reaction. The other two forms β-C and γ-C being less reactive resulted in the

deactivation of the catalyst with β-C being more significant in the deactivation process[30].

Catalyst performance like catalyst activity, stability and carbon deposition depends upon the different variables which include active material, support material, promoter effect, temperature, calcination temperature, particle size and preparation method which will be discussed in the later section.

2.4 Role of Parameters in DRM

The catalyst being used in DRM is affected by the number of parameters which may influence catalytic activity, stability, carbon deposition and the target product compositions. The role of parameters will be discussed in the following section.

2.4.1 Active Metals

Dry reforming of methane is practised with the noble and the non-noble metals but the noble metals (Ru, Rh, Pd, Pt and Ir) has shown superior activity, stability and coking resistance towards reforming processes. Among the noble metals, Ru and Rh show relatively higher catalytic activity compared to others[31]. In terms of catalytic activity, the noble metals show the trend Ru, Rh > Ir > Pt, Pd when operated at 550 °C -600 °C in DRM. However in terms of coking, the following trend was observed Ni>>> Rh>Ir, Ru>Pt, Pd at temperature of 500 °C[32, 33]. For the sake of industrial application, Ru is more suitable than Rh because of the less cost. Tsyganok et al.[34] Investigated the effect of noble metals (Ru, Rh, Pd, Pt and Ir) over Mg-Al layered doubled hydroxides and the results shown higher activity and stability for Ru, Rh and Ir over $MgAlO_x$ and also Ru shown the least coke deposition weightage among the noble metals over $MgAlO_x$. The coke deposition decreasing trend was observed as follows: Pd/ $MgAlO_x$>Au/ $MgAlO_x$>Pt/ $MgAlO_x$>Ir/ $MgAlO_x$>Rh/ $MgAlO_x$>Ru/ $MgAlO_x$. The X-ray diffraction (XRD) pattern and the transmission electron microscopy (TEM) image of the Ru based catalyst as shown in Fig.2.3 show structure of the catalyst before and after dry reforming at 800 °C for 50 h. The spent catalyst show the presence of MgO and $MgAl_2O_4$ but absence of Ru which depict the dispersion of small metal particles and is the evidence of higher catalytic activity and lower carbon deposition.

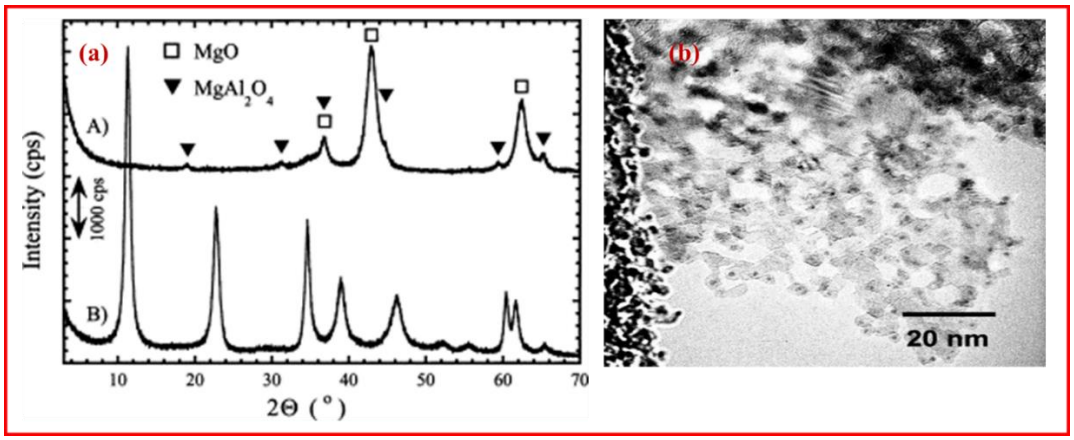

Fig 2.3 (a) XRD pattern of catalyst B) before and A) after activity test (b) TEM image of catalyst after activity test[34]

Although noble metals show superior catalytic activity and impressive resistance to coke deposition but are quite expensive for the use in the industrial applications. In comparison to noble metals (Ru, Rh, Pd, Pt and Ir) and non-noble metals (Ni and Co), non-noble metals show comparatively better catalytic activity results but coke deposition leading to deactivation is the problem with these type of catalysts[33]. For DRM, Ni based catalysts are most suitable. Hou et al.[35, 36] compared the Co and Ni catalysts onto Al_2O_3 support and found better results for Ni/Al_2O_3 in terms of catalytic activity and stability and the reason for that was highly dispersed small size Ni particles. Coke deposition in Ni-based catalyst is major issue but this can be sorted out by the addition of alkaline dopants, supports with basic properties and the addition of noble metals to highly dispersed Ni catalysts[37]. The researchers found interest in increasing the stability of the catalysts. Co based catalysts are also under study owing to their Ni like activity for the DRM reaction but the stability issues and deactivation is also associated with these types of catalyst. Although Co have limited contribution to DRM but the catalyst have the ability to present better stability to coke deposition. El et al.[38] investigated the confinement effects on the catalytic performance of two silica supports (SiO_2 and SBA-15) on Co loading. The results indicated that Co/SBA-15 showed stability against sintering of mesopores during DRM and addition of rhodium on Co/SBA-15 showed increased stability and activity with less carbon coking.

The focus of the study is to develop the Co based catalyst with better catalytic activity and stability for DRM process. For the Co catalysts, deactivation is mainly because of oxidation and carbon deposition which depends upon the loading of the Co. Highly loaded Co results in deactivation because of carbon deposition and low loading of Co results in oxidation leading to deactivation[39]. Similar results were identified by Jose-Alonso et al.[28] where 1% Co loaded catalyst showed deactivation due to oxidation while carbon deposition leading deactivation was found for 9% Co loaded catalyst. Some of the Co based catalyst used in DRM is listed in Table2.1

Table 2.1 List of Co based catalyst used in DRM

Metal	**Support**	**Preparation Method**	**Temp (°C)**	**Reactor Type**	**CH_4 conversion (%)**	**CO_2 conversion (%)**	**Ref.**
Co	γ-Al_2O_3	Sol-gel	800	FBR	32.0	39.0	[36]
Co	MgO	Impregnation	900	FBR	91.9	93.9	[40]
Co	γ-Al_2O_3	Impregnation	700	FBR	56.0	59.0	[41]
Co	SiO_2	Impregnation	850	FBR	12	31	[42]
Co	MCM-41	Surfactant assisted route	750	FBR	27	-	[43]
Ni-Co	CeO_2-ZrO_2	Solvothermal Approach	800	FBR	30	37	[44]

In addition, higher stability and catalytic activity has been reported to bimetallic catalysts as compared to monometallic catalyst. Carbon deposition can be inhibited by the use of bimetallic catalysts and in this regard small amount of noble metals addition to base active metal show very good results[19]. As noble metals are expensive so cobalt comes out to be good candidate to use for bimetallic catalysts owing to high melting temperature. Ni-Co alloy as bimetallic catalyst has shown improved catalyst activity and stability results compared to use of monometallic catalyst. Zhang et al.[45] shown that the higher metal dispersion and small particles size of the Ni-Co catalyst resulted in good catalytic performance and suppressed carbon formation. Similar results were observed for the use of Ni-Co catalyst onto TiO_2 support where improved

catalytic performance was observed as a result of resistance to metal oxidation[46]. So the synergetic effect of Co and Ni and the higher metal dispersion and small particles formation of bimetallic catalysts emphasizes the use of it.

2.4.2 Support

In DRM, the coke deposition is mainly due to the Boudouard reaction and the methane decomposition and this coke deposition is minimized by higher reaction temperature and the use of dilute reaction mixture which need the use of active metals, transition metals, supports and promoters to form catalyst. The resultant catalyst gets suitable against the carbon deposition. Moreover supports play key role in improving catalytic activity for dry reforming of methane. The nature of the support is very important in determining the activity and stability of the catalyst. $MgAl_2O_4$ is an excellent support as it provides both basic and acidic active sites and is found to be good resistant to sintering and possess high mechanical strength[45]. Moreover in case of DRM, the basic supports help in CO_2 dissociation while the acidic support helps in decomposition of CH_4[47]. $MgAl_2O_4$ is a combination of both basic MgO support and acidic Al_2O_3 support. Hadian et al.[48] observed the effect of Ni loadings on high surface $MgAl_2O_4$ support and found that with the increase in the loading, the catalytic activity improved while increasing the carbon deposition. The purpose of the basic support is to gasify carbon specie which help in carbon deposition suppression[49]. Ni was incorporated on basic MgO support and various catalysts with different loading were investigated for DRM off which Ni8-Mg6 shown higher methane conversion upto 84%. Moreover the formation of NiO-MgO increased the stability of the catalyst as shown by various studies[50, 51]. Brungs et al.[23] performed experiments using various supports on molybdenum carbide (Mo_2C) and find the trend of the stability as follows: $Mo_2C/Al_2O_3 > Mo_2C/ZrO_2 > Mo_2C/SiO_2 > Mo_2C/TiO_2$. Higher metal support interaction for the Mo_2C/Al_2O_3 catalyst was the reason behind higher stability however the in process oxidation caused deactivation due to formation of molybdenum oxide. In comparison of both MgO and Al_2O_3 supports, experiments were done and the results shown that for only Ni used, Ni/ Al_2O_3 exhibited higher catalytic activity than Ni/MgO but using NiO, NiO/MgO provided higher catalytic activity and stability compared to NiO/Al_2O_3[52, 53]. However MgO is a basic support and comes out on top in suppressing carbon deposition.

To improve catalytic performance, the use of bi-support catalysts is very effective. In this regard TiO_2 is another excellent support which shows good results in carbon deposition suppression[54]. Structured TiO_2 improves the catalytic activity and stability[55]. Seo et al.[54] performed experiment by using bare Ni and then by addition of TiO_2 support to it and found that that Ni/TiO_2 showed higher methane and carbon dioxide conversion with higher stability. Moreover due to higher carbon dioxide conversion, higher coking resistance was observed for Ni/TiO_2 compared to the use of bare Ni. Bradford and Vannice [56]used SiO_2 and TiO_2 supports on various metals (Cu, Co, Fe, Ni, Ru, Rh, Ir, Pt and Pd) and found that TiO_2 shows higher catalytic activity compared to SiO_2 which is due to higher metal support interaction and formation of TiO_x specie as a result of reduction which causes the destruction of large-size ensembles. Takanabe et al.[46] also used TiO_2 support on different metals and found similar results. Some of the supports used in DRM are listed below in Table.2.2.

Table 2.2 List of some supports used in DRM

Metal	**Support**	**Preparation Method**	**Temp (°C)**	**Reactor Type**	**CH_4 conversion (%)**	**CO_2 conversion (%)**	**Ref.**
Ni	Al_2O_3	Impregnation	700	FBR	63.0	57.3	[53]
NiO	Al_2O_3	Impregnation	800	FBR	52.5	-	[57]
Ni	MgO	Wetness Impregnation	700	FBR	20.0	30.0	[52]
NiO	MgO	Impregnation	800	FBR	82.0	90.0	[58]
Ru	Al_2O_3	Impregnation	750	FBR	46.0	48.0	[59]
Rh	Al_2O_3	Impregnation	500	FBR	7.7	13.5	[60]
Rh	MgO	Impregnation	800	FBR	80.3	85.8	[61]
Rh	TiO_2	Impregnation	800	FBR	33.1	46.5	[61]

2.4.3 Promoter

Promoters play key role in improving catalyst activity and stability and are of great importance in dealing with carbon deposition issues. Promoters enhance the catalyst stability by modifying the surface structure of the catalyst. Promoters enhance the metal dispersion over the support by the strong metal support interaction effect and causes the bending of the catalyst state to more basic sites[62]. Basically promoters have two major roles when interacted with metal: (1) blocking the sites on metal surface which promote carbon nucleation and growth by enhancing metal dispersion and keeps the particles size small. (2) gasify the coke formed to avoid coke deposition[63].

San Jose-Alonso et al.[64] studied the promotional effect of K on Co/γ-Al_2O_3 and results shown lower coke deposition however the catalytic activity reduced. The reduction in conversions of reactants was due to the promotion in gasification of coke and the covering of active sites of cobalt for methane decomposition. York et al.[65] discussed the effect of Molybdenum (Mo) and tungsten (W) promoters on 2% Ni/Al_2O_3 and the results indicated decrease in coke deposition with the promotion of catalyst with Mo however the methane and carbon dioxide conversion shown no effect. With the use of W promoter, slight decreased conversion was observed but had the stable activity results.

The weight percentage of the promoter added also plays key role in enhancing catalytic activity, stability and preventing coke deposition. Daza et al.[66] investigated the effect of Ce with different weight% (0, 1, 3, 5 and 10wt %) on Ni/Mg-Al and found its significant effect in coke deposition inhibition however catalytic activity shown no significant effect with the promotion of Ce. The maximum catalytic activity was observed for the catalyst with the use of 3% Ce and 100 h stability for reforming reaction. In another study the promotional effect of yttrium (Y) and its oxide on Ni/ γ-Al_2O_3 and Pd/Al_2O_3 was investigated which improved catalytic performance and strong metal-support interaction. Small particles formation suppressed sintering and coke deposition[67, 68]. Another study investigated the use of Sn, Ce, Mn and Co promoters on Ni/MgO. The results shown the higher catalytic activity and stability results by the use of Co promoter while Ce and Mn shown lower activity results. Additionally higher resistance to coke deposition was observed for Sn and Co

promoted catalysts. The reason behind higher activity for Co is its affinity to oxygen species[69].

Similarly the use of K promoter on Ni/Al_2O_3 in another study shown higher activity results and higher inhibition to coke deposition when compared by using other promoters (Ca,Mn and Sn). This promotional effect of K is due to higher metal support interaction due to formation of small particles and enhanced gasification of coke[70]. Ngaraja et al.[71] studied the effect of K promoter over $Ni/MgO-ZrO_2$ and the results shown higher catalytic activity and stability results with 0.5% K promoted catalyst.

Some promoters that has been added to the catalysts used in DRM process has been listed down in Table2.3. Moreover the proper selection of promoters, their suitable addition of weight percentage to the catalyst is very important in improving catalytic performance. Promoters play key role in reduction of the catalysts, enhancing metal-support interaction, in formation of smaller particles and also the number of the basic active sites increase with the use of promoters.

Table 2.3 List of some promoters used in DRM

Metal	**Support**	**Promoter**	**Promoter wt (%)**	**CH_4 conversion (%)**	**CO_2 conversion (%)**	**Ref.**
Ni	Al_2O_3	Unpromoted	*	63.0	57.3	[53]
		ZrO_2	10	71.3	62.1	
Ni	CeO_2	Unpromoted	*	11.7	29.7	[72]
		K	0.5	4.9	29.9	
Rh	Al_2O_3	TiO_2	5	13.7	19.6	[60]
			10	11.2	19.4	
Ni	γ- Al_2O_3	Unpromoted	*	73.0	79.0	[73]
		Ca	0.05	73.6	80.3	
		Zr	0.05	73.0	76.7	
		Ce	0.05	73.8	81.4	

Metal	Support	Promoter	Promoter wt (%)	CH_4 conversion (%)	CO_2 conversion (%)	Ref.
Ni	MgO	Unpromoted	*	70.0	83.0	[69]
		Sn	1.46	20.0	25.0	
		Ce	0.58	71.0	83.0	
		Mn	2.47	4.0	7.00	
		Co	0.51	73,0	90.0	
Ni	γ- Al_2O_3	Unpromoted	*	28.5	5.8	[67]
		Y_2O_3	5	77.5	64.3	
			8	87.1	68.0	
			10	91.8	73.9	
Ni	SBA-15	MgO	3	97.8	96.9	[74]
Ni/Mo	SBA-15	Unpromoted	*	84	96	[75]
		La_2O_3	2	98	95	
Ni	γ- Al_2O_3	Unpromoted	*	80.0	90.0	[76]
		CeO_2	5	79.0	88.0	
			10	78.0	86.0	
			15	77.0	85.0	
Ni	MCM-41	Unpromoted	*	52.0	-	[77]
		Ti	1	2.0	-	
		Mn	1	4.0	-	
		Zr	1	91.0	-	

In the above table, the promotional effect of the promoter have been shown on the catalytic activity of catalyst.

2.4.4 Influence of Preparation Method

Catalyst preparation method is an important aspect as catalyst properties and the performance of catalyst largely dependent on it[78]. Catalyst structure and its behaviour in catalytic performance tests depend on type of preparation method, pre-treatment processes, precursor and solvent concentration, calcination temperature and PH maintained. So proper catalyst preparation method is necessary in order to achieve higher catalytic performance. In this regard, a lot of catalyst preparation techniques has been used up to date and work is being done in search of more unique and better preparation method.

Pt/ZrO_2 catalyst promoted with Ce was prepared using sequential impregnation and coprecipitation method and the comparative results shown that the catalyst prepared with coprecipation method exhibited higher methane and carbon dioxide conversions for DRM process[79]. Moreover higher performance was due to well interacted Pt-Ce with highly dispersed Pt particles resulting lower carbon deposition. Compared to other preparation methods, plasma treatment has dominant effect on catalyst preparation. This effect was shown by Rahemi et al.[80] who prepared Ni/Al_2O_3 and Ni/Al_2O_3-ZrO_2 by using impregnation and plasma treatment method. The results indicated higher methane and carbon dioxide conversions for Ni/Al_2O_3-ZrO_2 treated with plasma and the Ni particles were found to be highly dispersed and small sized.

Similarly plasma treatment in place of thermal calcination produced catalysts with good properties which aid in higher catalytic performance. Odedairo et al.[81] prepared Ni/CeO_2 by using impregnation method and then used both thermal calcination and microwave plasma treatment in place of thermal calcination separately and the comparative results exhibited higher catalytic activity and stability for the plasma treated catalyst. Different catalysts were tested using only impregnation preparation method and also impregnation leading to plasma treatment. Plasma treated catalysts shown good activity and stability results and shown properties of anti-coking, high dispersion, small particles formation and strong metal support interaction[80, 82, 83]. However the disadvantage linked with plasma treatment is large amount of energy consumption.

In another study, effect of combined use of sol-gel and critical drying was tested. In this regard Ni/Al_2O_3 was prepared using sol-gel supercritical drying and also with the impregnation method. The catalyst prepared with sol-gel supercritical drying show properties of high surface area with highly dispersed small sized particles and good metal-support interaction and catalytic activity results[35]. Ni/Al_2O_3 was also tested with precipitation, impregnation, sol-gel and supercritical drying and multi-bubble sonoluminescence (MBSL). The comparative results show higher activity and stability results with low carbon deposition by using MBSL catalyst preparation method owing to nanoparticles formation[84]. Another catalyst preparation method which has significant advantage over other preparation methods in nanoparticles formation is Micro-emulsion (ME) which uses mixture of transparent nano-sized water droplets in oil stabilized by surfactant[85].

Novel catalyst preparation methods include core-shell catalysts which can deal with the carbon deposition issues in DRM process. Moreover to have the better control over catalyst composition, particles size, developments in the synthesis of yolk-shell catalyst is under process[86]. Since catalyst preparation methods effect catalytic performance, particles size and dispersion, metal-support interaction and coke deposition. So the proper selection of preparation method helps in achieving higher catalytic activity and stability, higher dispersion, small sized particles, better metal-support interaction and good anti-coke properties. Below are few of the catalysts listed in Table2.4 which are prepared using different preparation techniques. The catalysts have been prepared using different techniques in different operating conditions and set of metal and supports. The below table shows the effect of the preparation methods through which the catalyst have been synthesized. There are a number of preparation methods of catalyst each having its own pros and cons as one preparation method stands good for one type of catalyst while the other preparation method holds good for the other type of catalyst and the condition of the preparation method has also significant effect on catalyst final properties. The preparation method effects the catalyst properties which eventally effects the catalytic performance of the catalyst and the convertion rates of the reactant. Mostly used methods are the impregnation method and coprecipitation method.

Table 2.4 Preparation methods effect on DRM activity

Metal	Support	Preparation Method	Temp (°C)	CH_4 conversion (%)	CO_2 conversion (%)	Ref.
Ni	CeO_2	Impregnation	700	17.0	40.0	[81]
		Impregnation		37.0	70.0	
Ni	MgO	Impregnation	700	20.0	30.0	[52]
		Impregnation		49.0	54.0	
Ni	γ- Al_2O_3	Impregnation	700	44.0	48.0	[82]
		Impregnation		52.0	59.0	
Co	γ- Al_2O_3	Impregnation	700	56.0	59.0	[41]
Ni	γ- Al_2O_3	Impregnation	750	72.0	80.0	[83]
		Impregnation		80.0	85.0	
NiO	Al_2O_3	Impregnation	800	59.0	52.0	[57]
NiO	MgO	Impregnation	800	82.0	90.0	[58]
NiO	MgO	Co-precipitation	600	26.0	30.0	[87]
Ni	SiO_2	Micro-emulsion	800	60.0	73.5	[88]
Co	γ- Al_2O_3	Sol-gel and supercritical drying	800	32.0	39.0	[36]

2.4.5 Influence of Calcination Temperature

Calcination temperature is one of the important factors which activate the catalyst to become reactive and stable[89]. The reactivity and stability of the catalyst depends upon the calcination temperature to control the size of the particles[90]. For complete salts decomposition, calcination of precursors deposited is of importance. Also the

solid state reactions and transformations occurs as a result of calcination. Calcination temperature is critical in catalyst synthesis so a lot of catalysts have been synthesized and effect of calcination temperature has been studied.

Mguni et al.[91] used the calcination temperatures in range of 500-800 °C for MgO and observed higher activity and smaller particle sizes at 500-700 °C while at 800 °C the activity decreased due to sintering of MgO resulting increase of crystallite size. Yang et al.[92] studied different calcination temperatures (350, 450, 570 °C) for 5% CoO_x/TiO_2 and found that higher CO conversion (82%) and higher activity results were noted at 450 °C compared to other two calcination temperatures. The Co species so formed at 450 °C were of clean Co_3O_4 while at 570 °C, lower conversion was attributed to Co_3O_4 covered by Co_nTiO_{n+2} and 350 °C was not sufficient temperature for complete decomposition of precursor.

The calcination temperature in some cases is high because of incomplete decomposition at lower calcination temperatures while in some cases stabilities are induced in catalyst at even lower calcination temperature and lower metal loading in catalyst. Also the suitable calcination duration is important to achieve higher stability and activity of the catalysts. Brungs et al.[23] studied the effect of calcination duration for Mo_2C catalyst and found that 4 h calcination duration got better stability results compared to the one calcined for 24 h.

In another study it was noted that increase in calcination temperature tends to decrease the surface area. For Co/ γ- Al_2O_3 calcined at 500 °C and 1000 °C it was observed that at 500 °C formation of Co_3O_4 with lower cobalt content (6%) resulted in higher conversion and lower coke formation while the one calcined at 1000 °C formed $CoAl_2O_4$ and Co_2AlO_4 species with higher cobalt content (9%) resulting in higher conversions and lower carbon depositions[93]. The results indicate that one calcination temperature is suitable to certain metal content. In case of DRM, the effect of the calcination temperature on the catalytic activity of the catalysts is listed down in Table2.5. Some of the important metal supported catalysts have been mentioned in the below table which show the effect of calcination temperature, calcination time on the conversion rates of carbon dioxide and methane along with the preparation method used for catalyst synthesis.

Table 2.5 Calcination temperature effect on catalytic activity in DRM

Metal	Support	Preparation method	Calcination condition		CH_4 conversion (%)	CO_2 conversion (%)	Ref.
NiO	MgO	Impregnation	600	1.5	82.0	90.0	[58]
			800		93.0	95.0	
Co	MgO	Impregnation	500	8	95.7	97.4	[40]
			800		91.9	93.9	
			900		5.5	11.9	
Ni	Al_2O_3	Wetness Impregnation	800	4	91.2	70.6	[67]
Ni	Al_2O_3	Sol-gel	850	10	84.7	90.8	[94]
Ni	γ- Al_2O_3	Wetness Impregnation	600	2	68.0	66.4	[95]
			900		73.0	80.1	
La_2NiO_4	γ- Al_2O_3	Sol-gel	500	6	60.0	49.5	[96]
			800		49.0	60.0	

Calcination temperature and calcination during is of critical importance because above and below the temperature limits of calcination, deactivation or drop in activity results occur. For DRM, it is suggested to calcine catalyst at high temperature because dry reforming requires high temperature of reaction to obtain acceptable conversions. Therefore proper selection of calcination temperature is important to obtain good activity and stability results.

2.4.6 Influence of Reactor Type

The optimization of the catalyst bed is another way for effective catalytic performance in place of usage of carbon resistant catalysts[15]. In this regard many reactor setups like fixed bed reactor (FBR), fluidized bed reactor (FIBR), micro reactor, magnetized fluidized bed reactor (MFIBR), hollow fiber membrane reactor (HMFR) and other

reactor systems have been used up to date. Single and multi-mode switching have been tested for NiO/Al_2O_3 catalyst for fixed/fluidized bed and the results indicated higher methane and carbon dioxide conversions for FIBR compared to FBR in single mode while for multimode switching drop in carbon deposition was spotted during FBR to FIBR switching which indicates that FIBR is more effective than FBR in carbon deposition and higher catalytic activity[97].

Another reactor used to improve the fluidization quality of nanoparticle catalysts is by application of magnetic field to FIBR and the reactor is named as MFIBR[98]. With 20% Co/Al_2O_3 catalyst in dry reforming, the results for methane conversion, carbon dioxide conversion and carbon deposition resistance were in order: MFIBR>FIBR>FBR[36]. Membrane reactor has the advantage of less temperature operation with less catalyst and the single step production and separation of H_2 from the products[99]. Similarly HFBR and tubular membrane reactor (TMR) were used for the performance comparison with FBR onto Pd/Al_2O_3 catalyst and the results for methane conversion were superior for HFBR compared to FBR while no significant difference was observed for HFBR and TMR in methane conversion[100]. Additionally pure H_2 produced free of CO_x is the associated advantage with use of HFBR.

On industrial scale, higher pressures are used for dry reforming therefore the design of high pressure reactor with suitable catalyst is important. The unfavourable parameters of high pressure and low temperature effect the chemistry of DRM resulting in higher carbon deposition, lower catalytic activity and lower H_2 selectivity and yield. These results were shown by Takahashi et al.[101] where mesoporous $Pt/SO\text{-}ZrO_2$ catalyst and non-porous Pt/ZrO_2 catalyst were investigated for DRM in high pressure FBR reactor. Although mesoporous $Pt/SO\text{-}ZrO_2$ shown comparable higher methane (17%) and carbon dioxide (29%) conversion when compared to non-porous Pt/ZrO_2 with lower methane (14%) and carbon dioxide (26%) conversion but the overall lower catalytic activity and higher coke formation was due to high pressure and lower temperature used. Some of the reactors used in DRM have been listed down in Table2.6. The type of reactor usage for the reforming process has the major influence on the final catalytic activity results.

Table 2.6 Effect of reactor type used on catalytic activity in DRM

Metal	Support	Reactor	Reaction Temp (°C)	CH_4 conversion (%)	CO_2 conversion (%)	Ref.
Ni	SiO_2	FBR	750	47.0	60.0	[102]
		FIBR		49.0	64.0	
Ni	Al_2O_3	TFBR	700	60.0	70.0	[103]
Ni	γ- Al_2O_3	FBMR	800	89.0	94.0	[49]
Ni	Al_2O_3	DCBR	900	42.0	70.0	[104]
Ru	ZrO_2-La_2O_3	HFMR	525	23.0	-	[100]
		TMR	450	25.0	-	
		FBR	475	13.0	-	
Ni	Al_2O_3	MR	700	74.1	81.0	[65]
Ni	Al_2O_3	FBCR	700	72.5	69.0	[105]
Ni	MgO	FIBR	800	64.0	-	[106]
		FBR	850	50.0	62.0	
Pt	MgO	FIBR	800	57.0	-	[106]
		FBR	850	40.0	50.0	

where TFBR: tubular fixed bed reactor; FBMR: fixed bed quartz micro reactor; DCBR: direct contact bubble reactor; HFMR: hollow fiber membrane reactor; TMR: tubular membrane reactor; MR: micro reactor; FBCR: fixed bed continuous flow reactor; SFFR: solar power fluid- wall aerosol flow reactor.

The reactors comparison on the basis of performance have been studied. Compared to micro reactors, tubular FBR shown higher conversion rates while fluidized bed micro reactor shown higher catalytic activity than fixed bed micro reactor[65, 105]. Solar reactors show higher conversions with no catalyst because of high temperature but the issue is solar energy storage[107]. In this regard a reactor named direct contact bubble

reactor is used which resolve storage problem. AL-Ali et al.[104] used DCBR reactor for DRM with 40% methane conversion and 70% carbon dioxide conversion.

A number of reactors are currently being used for DRM while FIBR has shown favourable conversions and catalytic activity for DRM reaction but the use of the reactor depends upon the reaction conditions, reaction type and the requirements because every reactor have some advantages and disadvantages associated with them.

2.5 Catalyst Preparation Methods

Catalyst preparation methods are influential in catalytic performance of the catalyst. As the preparation techniques of the catalyst include certain steps such as precursors, solvent concentration, calcination temperature, PH and aging time which directly affect the properties of the final prepared catalyst[108]. The performance of the catalyst depends upon the properties of the catalyst. Catalyst is prepared by various methods but the most common methods include impregnation method, precipitation and co-precipitation method, hydrothermal method, sol-gel method, surfactant-assisted methods and advanced preparation methods.

2.5.1 Impregnation Method

Impregnation method usually relates with adsorption method and the ion exchange method and in this method interaction of metal and support by impregnation affect the final catalyst properties[109]. Impregnation is the mixing of porous support into solution of active metal precursor which is then dried to obtain supported catalysts. In wet impregnation method, excess of solution is used while the incipient wetness impregnation method also known as dry impregnation uses appropriate concentrated volume of solution which is equal or slightly less than support pore volume.

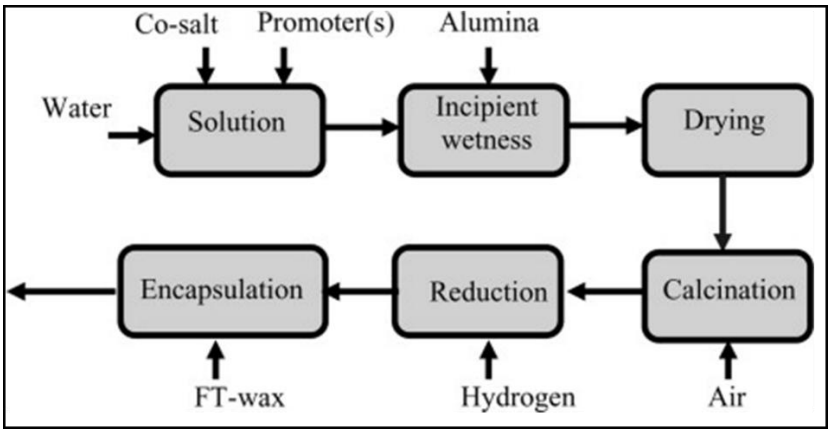

Fig 2.4 Incipient wetness impregnation steps

In incipient wetness impregnation method, capillary action mechanism is used while it changes to diffusion process in wet impregnation method[110]. The temperature and the precursor concentration are the factors which affect the preparation of catalyst by impregnation. The impregnation method is fast, easy and have good control over catalyst structures and properties. Incipient wetness impregnation process is shown in Fig 2.4.

2.5.2 Precipitation or Co-precipitation Method

Precipitation type method is mostly used type of catalyst preparation method for the single, mixed and supported catalysts[111]. Precipitation method has certain parameters like temperature, salt concentration, PH adjustment and evaporation. The change of the conditions result change in crystal growth and aggregation. The size and structure of the catalysts change as a result of change of conditions which ultimately affect the catalyst properties and in result the catalyst performance.

Precipitation method follows four major steps in catalyst preparation as shown in Fig 2.5:

i. Dissolution: salts are dissolved in water or other medium to form homogeneous solution.
ii. Precipitation: PH adjustment and evaporation to form precipitates resulting salts into hydroxide or oxide forms.
iii. Filtration and drying: solid precipitate is collected, dried and grinded to powder form.
iv. Calcination: calcined powder to convert any hydroxides into oxides.

The catalyst resulted of precipitation method has fine uniform particles with less agglomeration but the precipitation methods lack control of the solid phase nucleation and growth process[112].

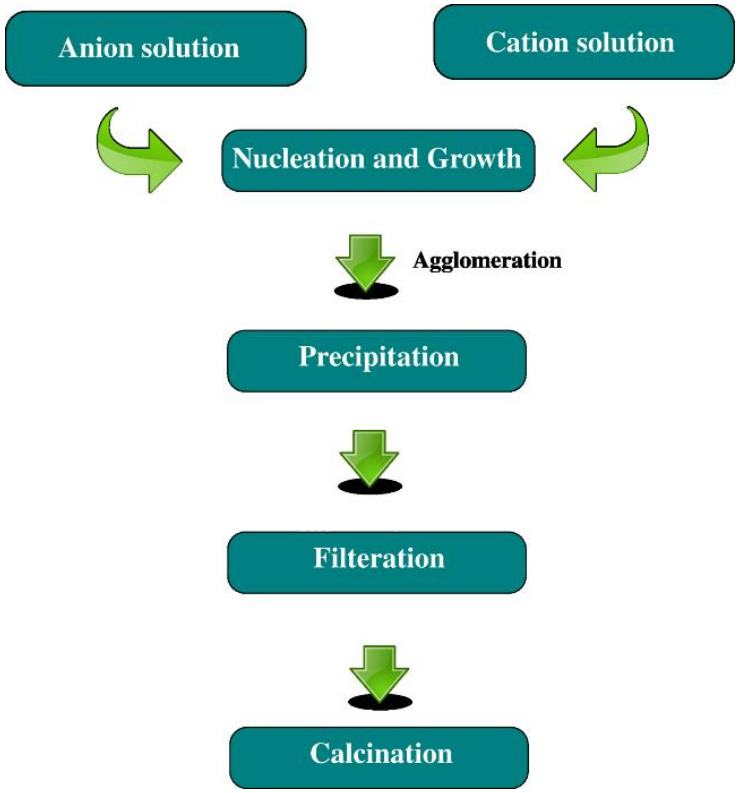

Fig 2.5 Co precipitation process steps

2.5.3 Hydrothermal Method

Hydrothermal method is another preparation method which uses aqueous solution in the hydrothermal reactor also known as closed reaction vessel to carry out the reaction. The crystals are formed by high temperature high pressure reaction conditions by heating the hydrothermal reactor[113]. The main steps included in hydrothermal preparation method are shown in Fig 2.6:

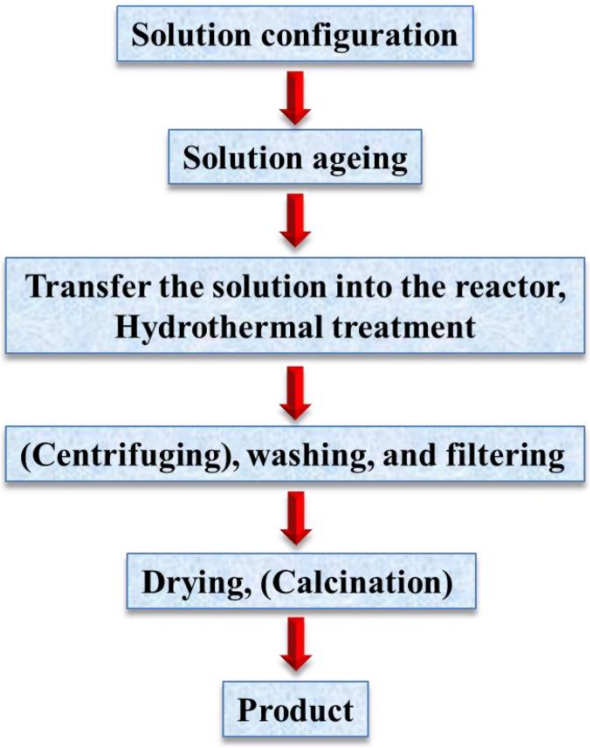

Fig 2.6 Hydrothermal process Steps

The crystal growth is an important factor in catalyst preparation and crystal growth in hydrothermal method depends upon the hydrothermal conditions. So better crystal growth with suitable treatment conditions result in catalyst with better catalytic performance.

2.5.4 Sol-Gel Method

Sol-gel method is very effective method for metal dispersion over support. The sol-gel method has better control over the composition, homogeneity, texture and structural properties of the solids. A large number of operation procedures for sol-gel method are usually followed but the common steps of preparations[114] include:

i. Dissolved precursor's conversion to reactive state.
ii. Polycondensation of activated precursors to nanoclusters.
iii. Gelation
iv. Aging
v. Washing
vi. Drying

Sol-gel is an appropriate method for the preparation of mixed metal oxides. Sol-gel method has the advantages of highly control, homogeneity and molecular scale mixing of constituents associated with it. The process of sol-gel is shown in Fig 2.7.

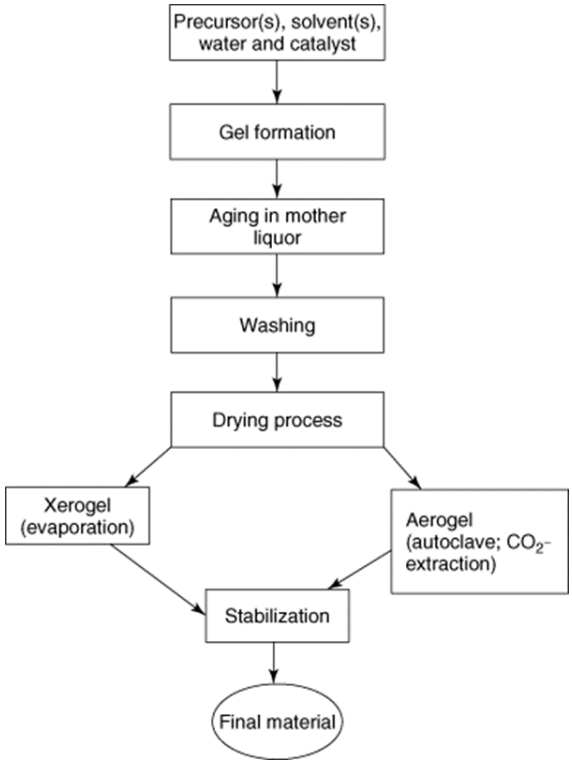

Fig 2.7 Sol gel process steps

2.5.5 Surfactant-Assisted Methods

Surfactant assisted methods are the other type of preparation method in which surfactants are added for growth regulation and fine particle sizing of nanoparticles in aqueous-based solutions[115]. The surfactants are added in the sol-gel preparation, sol-gel preparation and other suitable preparation methods in order to prepare catalyst having better properties. There are many types of surfactants used like glycol, CTAB (cetyl trimethyl ammonium bromide) and polyol etc.

Surfactants so added enhance the basicity which make the catalyst better coke resistant. Additionally the reduction behaviour of the surfactant added catalysts also gets improved.

2.5.6 Advanced Preparation Method

The catalyst preparation method has stepped up to the advanced level where the conventional preparation methods has been added with the plasma treatment. The

synergetic effect of the plasma and catalysis brought the major revolution in catalyst synthesis and development is being done in this effective approach of catalyst preparation[80].

The catalyst treated with plasma form highly dispersed particles with better metal-support interaction and small particle size with better properties. The prepared catalysts also show good results in catalytic performance and anti-coking[AK2][80, 116].

Summary

Greenhouse gases owing to their increasing amount in environment find different techniques to capture, store and recycle them to produce synthetic fuels. Syngas is being used as feed in production of fuels, chemicals and hydrocarbons and can be produced using various techniques among which catalytic reforming is of much importance. SRM, DRM, POM, auto thermal and tri-reforming are used in syngas production however DRM has advantage of employing both GHGs as feed and producing syngas in unity proportion which is important in Fischer-Tropsch (FT) synthesis leading to GLT applications.

The different parameters used in catalyst synthesis effect DRM catalytic performance. Among active metals, noble metals have superior performance but uneconomical while among non-noble metals Ni has shown good results for DRM and Co find limited application in DRM. The focus of study is to have good activity and stability results for DRM using Co metal. Similarly supports and promoters play key role in achieving good activity and stability results while depressing coke formation. Among different supports, $MgAl_2O_4$ with both acidic and basic nature contribute more towards DRM activity performance while TiO_2 provides excellent stability with good anticoking properties. Other parameters which effect the catalytic performance include calcination temperature, reactor type used and the catalyst preparation method each showing significant changes in results using different combinations and different conditions. So achieving good catalyst results need proper selection of conditions.

Among the catalyst preparation methods, various methods include impregnation method, co-precipitation method, hydrothermal method, sol-gel method, surfactant

assisted and plasma treated method. Among all, plasma treatment method show good results but consumes excess energy. All preparation methods are good for specific type of catalysts each while improving the nanoparticles properties important for achieving good catalytic activity results.

References

1. De Coninck, H., et al., *The acceptability of CO_2 capture and storage (CCS) in Europe: An assessment of the key determining factors: Part 1. Scientific, technical and economic dimensions.* International Journal of Greenhouse Gas Control, 2009. **3**(3): p. 333-343.
2. Hanif, A., T. Suhartanto, and M. Green. *Possible utilisation of CO_2 on Natuna's gas field using dry reforming of methane to syngas (CO & H_2).* in *SPE Asia Pacific Oil and Gas Conference and Exhibition*. 2002. Society of Petroleum Engineers.
3. Styring, P., et al., *Carbon Capture and Utilisation in the green economy*. 2011: Centre for Low Carbon Futures New York.
4. Lunsford, J.H., *Catalytic conversion of methane to more useful chemicals and fuels: a challenge for the 21st century.* Catalysis today, 2000. **63**(2-4): p. 165-174.
5. Pen, M., J. Gomez, and J.G.a. Fierro, *New catalytic routes for syngas and hydrogen production.* Applied Catalysis A: General, 1996. **144**(1-2): p. 7-57.
6. Spath, P.L. and D.C. Dayton, *Preliminary screening--technical and economic assessment of synthesis gas to fuels and chemicals with emphasis on the potential for biomass-derived syngas*. 2003, National Renewable Energy Lab., Golden, CO.(US).
7. El-Nagar, R.A. and A.A. Ghanem, *Syngas Production, Properties, and Its Importance*, in *Sustainable Alternative Syngas Fuel*. 2019, IntechOpen.
8. Dananjayan, R.R.T., P. Kandasamy, and R. Andimuthu, *Direct mineral carbonation of coal fly ash for CO_2 sequestration.* Journal of cleaner production, 2016. **112**: p. 4173-4182.
9. Chung, W.-C. and M.-B. Chang, *Review of catalysis and plasma performance on dry reforming of CH_4 and possible synergistic effects.* Renewable and Sustainable Energy Reviews, 2016. **62**: p. 13-31.

10. Gangadharan, P., K.C. Kanchi, and H.H. Lou, *Evaluation of the economic and environmental impact of combining dry reforming with steam reforming of methane.* Chemical Engineering Research and Design, 2012. **90**(11): p. 1956-1968.
11. Carvalho, L.S., et al., *Preparation and characterization of Ru/MgO-Al_2O_3 catalysts for methane steam reforming.* Catalysis Today, 2009. **142**(1-2): p. 52-60.
12. Oyama, S.T., et al., *Dry reforming of methane has no future for hydrogen production: Comparison with steam reforming at high pressure in standard and membrane reactors*. International journal of hydrogen energy, 2012. **37**(13): p. 10444-10450.
13. Olah, G.A., et al., *Bi-reforming of methane from any source with steam and carbon dioxide exclusively to metgas ($CO–2H_2$) for methanol and hydrocarbon synthesis.* Journal of the American Chemical Society, 2013. **135**(2): p. 648-650.
14. Asencios, Y.J. and E.M. Assaf, *Combination of dry reforming and partial oxidation of methane on NiO–MgO–ZrO_2 catalyst: effect of nickel content.* Fuel processing technology, 2013. **106**: p. 247-252.
15. Wurzel, T., S. Malcus, and L. Mleczko, *Reaction engineering investigations of CO_2 reforming in a fluidized-bed reactor*. Chemical engineering science, 2000. **55**(18): p. 3955-3966.
16. Ahmadpour, J. and M. Taghizadeh, *Catalytic conversion of methanol to propylene over high-silica mesoporous ZSM-5 zeolites prepared by different combinations of mesogenous templates.* Journal of Natural Gas Science and Engineering, 2015. **23**: p. 184-194.
17. Al-Sobhi, S.A. and A. Elkamel, *Simulation and optimization of natural gas processing and production network consisting of LNG, GTL, and methanol facilities.* Journal of Natural Gas Science and Engineering, 2015. **23**: p. 500-508.
18. Barelli, L., et al., *Hydrogen production through sorption-enhanced steam methane reforming and membrane technology: a review*. Energy, 2008. **33**(4): p. 554-570.

19. Chen, W.-H., *CO_2 conversion for syngas production in methane catalytic partial oxidation.* Journal of CO_2 Utilization, 2014. **5**: p. 1-9.
20. Wang, Y., et al., *Effect of Pr addition on the properties of Ni/Al_2O_3 catalysts with an application in the autothermal reforming of methane.* International journal of hydrogen energy, 2014. **39**(2): p. 778-787.
21. Snoeck, J.-W., G. Froment, and M. Fowles, *Steam/CO_2 reforming of methane. Carbon filament formation by the Boudouard reaction and gasification by CO_2, by H_2, and by steam: kinetic study.* Industrial & engineering chemistry research, 2002. **41**(17): p. 4252-4265.
22. Song, C. and W. Pan, *Tri-reforming of methane: a novel concept for catalytic production of industrially useful synthesis gas with desired H_2/CO ratios.* Catalysis Today, 2004. **98**(4): p. 463-484.
23. Brungs, A.J., et al., *Dry reforming of methane to synthesis gas over supported molybdenum carbide catalysts.* Catalysis Letters, 2000. **70**(3-4): p. 117-122.
24. de Araujo, G.C., et al., *Catalytic evaluation of perovskite-type oxide $LaNi1-xRuxO_3$ in methane dry reforming.* Catalysis Today, 2008. **133**: p. 129-135.
25. Kehres, J., et al., *Dynamical properties of a $Ru/MgAl_2O_4$ catalyst during reduction and dry methane reforming.* The Journal of Physical Chemistry C, 2012. **116**(40): p. 21407-21415.
26. Tsang, S., J. Claridge, and M. Green, *Recent advances in the conversion of methane to synthesis gas.* Catalysis today, 1995. **23**(1): p. 3-15.
27. Zhang, J., H. Wang, and A.K. Dalai, *Development of stable bimetallic catalysts for carbon dioxide reforming of methane.* Journal of Catalysis, 2007. **249**(2): p. 300-310.
28. San José-Alonso, D., M.J. Illán-Gómez, and M.C. Román-Martínez, *Low metal content Co and Ni alumina supported catalysts for the CO_2 reforming of methane.* International journal of hydrogen energy, 2013. **38**(5): p. 2230-2239.
29. Singh, R., et al., *Dry reforming of methane using various catalysts in the process.* Biomass Conversion and Biorefinery, 2019: p. 1-21.
30. Zhang, Z., et al., *Comparative study of carbon dioxide reforming of methane to synthesis gas over Ni/La_2O_3 and conventional nickel-based catalysts.* The Journal of Physical Chemistry, 1996. **100**(2): p. 744-754.

31. Jones, G., et al., *First principles calculations and experimental insight into methane steam reforming over transition metal catalysts.* Journal of Catalysis, 2008. **259**(1): p. 147-160.
32. Rostrup, N.J., *Process for the production of a reforming catalyst*. 1974, Google Patents.
33. Rostrupnielsen, J. and J.B. Hansen, *CO_2-reforming of methane over transition metals.* Journal of Catalysis, 1993. **144**(1): p. 38-49.
34. Tsyganok, A.I., et al., *Dry reforming of methane over supported noble metals: a novel approach to preparing catalysts.* Catalysis Communications, 2003. **4**(9): p. 493-498.
35. Hao, Z., et al., *Characterization of aerogel Ni/Al_2O_3 catalysts and investigation on their stability for CH_4-CO_2 reforming in a fluidized bed.* Fuel Processing Technology, 2009. **90**(1): p. 113-121.
36. Hao, Z., et al., *Fluidization characteristics of aerogel Co/Al_2O_3 catalyst in a magnetic fluidized bed and its application to CH_4–CO_2 reforming.* Powder Technology, 2008. **183**(1): p. 46-52.
37. Crisafulli, C., et al., *Ni–Ru bimetallic catalysts for the CO_2 reforming of methane.* Applied Catalysis A: General, 2002. **225**(1-2): p. 1-9.
38. El Hassan, N., et al., *Low temperature dry reforming of methane on rhodium and cobalt based catalysts: Active phase stabilization by confinement in mesoporous SBA-15.* Applied Catalysis A: General, 2016. **520**: p. 114-121.
39. Sukri, M.F.F., M. Khavarian, and A.R. Mohamed, *Effect of cobalt loading on suppression of carbon formation in carbon dioxide reforming of methane over Co/MgO catalyst.* Research on Chemical Intermediates, 2018. **44**(4): p. 2585-2605.
40. Wang, H. and E. Ruckenstein, *CO_2 reforming of CH_4 over Co/MgO solid solution catalysts—effect of calcination temperature and Co loading.* Applied Catalysis A: General, 2001. **209**(1-2): p. 207-215.
41. Zeng, S., et al., *Modification effect of natural mixed rare earths on Co/γ-Al_2O_3 catalysts for CH_4/CO_2 reforming to synthesis gas.* International journal of hydrogen energy, 2012. **37**(13): p. 9994-10001.

42. Song, S.-H., et al., *The influence of calcination temperature on catalytic activities in a Co based catalyst for CO_2 dry reforming.* Korean Journal of Chemical Engineering, 2014. **31**(2): p. 224-229.
43. Liu, D., et al., *A comparative study on catalyst deactivation of nickel and cobalt incorporated MCM-41 catalysts modified by platinum in methane reforming with carbon dioxide.* Catalysis Today, 2010. **154**(3-4): p. 229-236.
44. Črnivec, I.O., et al., *Effect of synthesis parameters on morphology and activity of bimetallic catalysts in CO_2–CH_4 reforming.* Chemical engineering journal, 2012. **207**: p. 299-307.
45. Zhang, J., H. Wang, and A.K. Dalai, *Effects of metal content on activity and stability of Ni-Co bimetallic catalysts for CO_2 reforming of CH4.* Applied Catalysis A: General, 2008. **339**(2): p. 121-129.
46. Takanabe, K., et al., *Titania-supported cobalt and nickel bimetallic catalysts for carbon dioxide reforming of methane.* Journal of Catalysis, 2005. **232**(2): p. 268-275.
47. Seo, H.O., *Recent scientific progress on developing supported Ni catalysts for dry (CO_2) reforming of methane.* Catalysts, 2018. **8**(3): p. 110.
48. Hadian, N., et al., *CO_2 reforming of methane over nickel catalysts supported on nanocrystalline $MgAl_2O_4$ with high surface area.* Journal of natural gas chemistry, 2012. **21**(2): p. 200-206.
49. Lucrédio, A.F., J.M. Assaf, and E.M. Assaf, *Methane conversion reactions on Ni catalysts promoted with Rh: Influence of support.* Applied Catalysis A: General, 2011. **400**(1-2): p. 156-165.
50. Wang, Y.-H., H.-M. Liu, and B.-Q. Xu, *Durable Ni/MgO catalysts for CO_2 reforming of methane: activity and metal–support interaction.* Journal of Molecular Catalysis A: Chemical, 2009. **299**(1-2): p. 44-52.
51. Hu, Y.H. and E. Ruckenstein, *Binary MgO-based solid solution catalysts for methane conversion to syngas.* Catalysis Reviews, 2002. **44**(3): p. 423-453.
52. Hua, W., et al., *Preparation of Ni/MgO catalyst for CO_2 reforming of methane by dielectric-barrier discharge plasma.* Catalysis Communications, 2010. **11**(11): p. 968-972.

53. Therdthianwong, S., C. Siangchin, and A. Therdthianwong, *Improvement of coke resistance of Ni/Al_2O_3 catalyst in CH_4/CO_2 reforming by ZrO_2 addition.* fuel processing technology, 2008. **89**(2): p. 160-168.
54. Seo, H.O., et al., *Carbon dioxide reforming of methane to synthesis gas over a TiO_2–Ni inverse catalyst.* Applied Catalysis A: General, 2013. **451**: p. 43-49.
55. Abbas, T., M. Tahir, and N.A. Saidina Amin, *Enhanced metal–support interaction in $Ni/Co_3O_4/TiO_2$ nanorods toward stable and dynamic hydrogen production from phenol steam reforming.* Industrial & Engineering Chemistry Research, 2018. **58**(2): p. 517-530.
56. Bradford, M.C. and M.A. Vannice, *The role of metal–support interactions in CO_2 reforming of CH_4.* Catalysis today, 1999. **50**(1): p. 87-96.
57. Chen, X., K. Honda, and Z.-G. Zhang, *A comprehensive comparison of CH_4-CO_2 reforming activities of NiO/Al_2O_3 catalysts under fixed-and fluidized-bed operations.* Applied Catalysis A: General, 2005. **288**(1-2): p. 86-97.
58. Feng, J., et al., *Calcination temperature effect on the adsorption and hydrogenated dissociation of CO_2 over the NiO/MgO catalyst.* Fuel, 2013. **109**: p. 110-115.
59. Djinović, P., et al., *Catalytic syngas production from greenhouse gasses: Performance comparison of Ru-Al_2O_3 and Rh-CeO_2 catalysts.* Chemical Engineering and Processing: Process Intensification, 2011. **50**(10): p. 1054-1062.
60. Sarusi, I., et al., *CO_2 reforming of CH_4 on doped Rh/Al_2O_3 catalysts.* Catalysis Today, 2011. **171**(1): p. 132-139.
61. Wang, H. and E. Ruckenstein, *Carbon dioxide reforming of methane to synthesis gas over supported rhodium catalysts: the effect of support.* Applied Catalysis A: General, 2000. **204**(1): p. 143-152.
62. Bezemer, G.L., et al., *Cobalt particle size effects in the Fischer− Tropsch reaction studied with carbon nanofiber supported catalysts.* Journal of the American Chemical Society, 2006. **128**(12): p. 3956-3964.
63. Yu, M., et al., *The promoting role of Ag in Ni-CeO_2 catalyzed CH_4-CO_2 dry reforming reaction.* Applied Catalysis B: Environmental, 2015. **165**: p. 43-56.

64. San José-Alonso, D., M. Illán-Gómez, and M. Román-Martínez, *K and Sr promoted Co alumina supported catalysts for the CO_2 reforming of methane.* Catalysis today, 2011. **176**(1): p. 187-190.
65. YORK, A.E., T. Suhartanto, and M.H. GREEN, *Influence of molybdenum and tungsten dopants on nickel catalysts for the dry reforming of methane with carbon dioxide to synthesis gas.* Studies in surface science and catalysis, 1998: p. 777-782.
66. Daza, C.E., et al., *High stability of Ce-promoted Ni/Mg–Al catalysts derived from hydrotalcites in dry reforming of methane.* Fuel, 2010. **89**(3): p. 592-603.
67. Sun, L., et al., *Effects of Y_2O_3-modification to Ni/γ-Al_2O_3 catalysts on autothermal reforming of methane with CO_2 to syngas.* International journal of hydrogen energy, 2013. **38**(4): p. 1892-1900.
68. Shi, C. and P. Zhang, *Effect of a second metal (Y, K, Ca, Mn or Cu) addition on the carbon dioxide reforming of methane over nanostructured palladium catalysts.* Applied Catalysis B: Environmental, 2012. **115**: p. 190-200.
69. Yu, M., et al., *Carbon dioxide reforming of methane over promoted NixMg1−xO (1 1 1) platelet catalyst derived from solvothermal synthesis.* Applied Catalysis B: Environmental, 2014. **148**: p. 177-190.
70. Juan-Juan, J., M. Román-Martínez, and M. Illán-Gómez, *Effect of potassium content in the activity of K-promoted Ni/Al_2O_3 catalysts for the dry reforming of methane.* Applied Catalysis A: General, 2006. **301**(1): p. 9-15.
71. Nagaraja, B.M., et al., *The effect of potassium on the activity and stability of Ni–MgO–ZrO_2 catalysts for the dry reforming of methane to give synthesis gas.* Catalysis today, 2011. **178**(1): p. 132-136.
72. Barroso-Quiroga, M.M. and A.E. Castro-Luna, *Catalytic activity and effect of modifiers on Ni-based catalysts for the dry reforming of methane.* International Journal of Hydrogen Energy, 2010. **35**(11): p. 6052-6056.
73. Al-Fatesh, A.S., A.H. Fakeeha, and A.E. Abasaeed, *Effects of selected promoters on Ni/Y-Al_2O_3 catalyst performance in methane dry reforming.* Chinese Journal of Catalysis, 2011. **32**(9-10): p. 1604-1609.

74. Huang, B., et al., *Effect of MgO promoter on Ni-based SBA-15 catalysts for combined steam and carbon dioxide reforming of methane.* Journal of natural gas chemistry, 2008. **17**(3): p. 225-231.
75. Huang, J., et al., *Carbon dioxide reforming of methane over Ni/Mo/SBA-15-La_2O_3 catalyst: Its characterization and catalytic performance.* Journal of natural gas chemistry, 2011. **20**(5): p. 465-470.
76. Chen, W., et al., *High carbon-resistance Ni/CeAlO_3-Al2O_3 catalyst for CH_4/CO_2 reforming.* Applied Catalysis B: Environmental, 2013. **136**: p. 260-268.
77. Liu, D., et al., *MCM-41 supported nickel-based bimetallic catalysts with superior stability during carbon dioxide reforming of methane: Effect of strong metal–support interaction.* Journal of Catalysis, 2009. **266**(2): p. 380-390.
78. Menegazzo, F., et al., *Optimization of bimetallic dry reforming catalysts by temperature programmed reaction.* Applied Catalysis A: General, 2012. **439**: p. 80-87.
79. Özkara-Aydınoğlu, Ş., E. Özensoy, and A.E. Aksoylu, *The effect of impregnation strategy on methane dry reforming activity of Ce promoted Pt/ZrO_2.* international journal of hydrogen energy, 2009. **34**(24): p. 9711-9722.
80. Rahemi, N., et al., *Synthesis and physicochemical characterizations of Ni/Al_2O_3–ZrO_2 nanocatalyst prepared via impregnation method and treated with non-thermal plasma for CO_2 reforming of CH_4.* Journal of Industrial and Engineering Chemistry, 2013. **19**(5): p. 1566-1576.
81. Odedairo, T., J. Chen, and Z. Zhu, *Metal–support interface of a novel Ni–CeO_2 catalyst for dry reforming of methane.* Catalysis Communications, 2013. **31**: p. 25-31.
82. Jin, L., et al., *CO_2 reforming of methane on Ni/γ-Al_2O_3 catalyst prepared by dielectric barrier discharge hydrogen plasma.* International journal of hydrogen energy, 2014. **39**(11): p. 5756-5763.
83. Zhu, X., et al., *Structure and reactivity of plasma treated Ni/Al_2O_3 catalyst for CO_2 reforming of methane.* Applied Catalysis B: Environmental, 2008. **81**(1-2): p. 132-140.

84. Kang, K.-M., et al., *Catalytic test of supported Ni catalysts with core/shell structure for dry reforming of methane.* Fuel Processing Technology, 2011. **92**(6): p. 1236-1243.

85. Boutonnet, M., S. Lögdberg, and E.E. Svensson, *Recent developments in the application of nanoparticles prepared from w/o microemulsions in heterogeneous catalysis.* Current Opinion in Colloid & Interface Science, 2008. **13**(4): p. 270-286.

86. Liu, J., et al., *Yolk/shell nanoparticles: new platforms for nanoreactors, drug delivery and lithium-ion batteries.* Chemical Communications, 2011. **47**(47): p. 12578-12591.

87. Zanganeh, R., M. Rezaei, and A. Zamaniyan, *Dry reforming of methane to synthesis gas on NiO–MgO nanocrystalline solid solution catalysts.* International journal of hydrogen energy, 2013. **38**(7): p. 3012-3018.

88. Li, Z., et al., *Yolk–satellite–shell structured Ni–yolk@ Ni@ SiO_2 nanocomposite: superb catalyst toward methane CO_2 reforming reaction.* Acs Catalysis, 2014. **4**(5): p. 1526-1536.

89. Montero, J.M., et al., *Structure-sensitive biodiesel synthesis over MgO nanocrystals.* Green chemistry, 2009. **11**(2): p. 265-268.

90. Chen, J., et al., *Influence of calcination temperatures of Feitknecht compound precursor on the structure of Ni–Al_2O_3 catalyst and the corresponding catalytic activity in methane decomposition to hydrogen and carbon nanofibers.* Applied Catalysis A: General, 2009. **362**(1-2): p. 1-7.

91. Mguni, L.L., et al., *Effect of calcination temperature and MgO crystallite size on MgO/TiO_2 catalyst system for soybean oil transesterification.* Catalysis Communications, 2013. **34**: p. 52-57.

92. Yang, W.-H., M.H. Kim, and S.-W. Ham, *Effect of calcination temperature on the low-temperature oxidation of CO over CoO_x/TiO_2 catalysts.* Catalysis today, 2007. **123**(1-4): p. 94-103.

93. Ruckenstein, E. and H. Wang, *Carbon deposition and catalytic deactivation during CO_2 reforming of CH_4 over Co/γ-Al_2O_3 catalysts.* Journal of Catalysis, 2002. **205**(2): p. 289-293.

94. Luna, A.E.C. and M.E. Iriarte, *Carbon dioxide reforming of methane over a metal modified Ni-Al_2O_3 catalyst.* Applied Catalysis A: General, 2008. **343**(1-2): p. 10-15.

95. Al-Fatesh, A. and A. Fakeeha, *Effects of calcination and activation temperature on dry reforming catalysts.* Journal of Saudi Chemical Society, 2012. **16**(1): p. 55-61.

96. Liu, B. and C. Au, *Carbon deposition and catalyst stability over La_2NiO_4/γ-Al_2O_3 during CO_2 reforming of methane to syngas.* Applied Catalysis A: General, 2003. **244**(1): p. 181-195.

97. Chen, X., K. Honda, and Z.-G. Zhang, *CO_2CH_4 reforming over NiO/γ-Al_2O_3 in fixed/fluidized-bed multi-switching mode.* Applied Catalysis A: General, 2005. **279**(1-2): p. 263-271.

98. Yu, Q., et al., *Enhanced fluidization of nanoparticles in an oscillating magnetic field.* AIChE Journal, 2005. **51**(7): p. 1971-1979.

99. Armor, J., *Catalysis with permselective inorganic membranes.* Applied catalysis, 1989. **49**(1): p. 1-25.

100. García-García, F., et al., *Dry reforming of methane using Pd-based membrane reactors fabricated from different substrates.* Journal of membrane science, 2013. **435**: p. 218-225.

101. Takahashi, Y. and T. Yamazaki, *Behavior of high-pressure CH_4/CO_2 reforming reaction over mesoporous Pt/ZrO_2 catalyst.* Fuel, 2012. **102**: p. 239-246.

102. Effendi, A., et al., *Characterisation of carbon deposits on Ni/SiO_2 in the reforming of CH_4–CO_2 using fixed-and fluidised-bed reactors.* Catalysis Communications, 2003. **4**(4): p. 203-207.

103. García-Diéguez, M., et al., *Characterization of alumina-supported Pt, Ni and PtNi alloy catalysts for the dry reforming of methane.* Journal of Catalysis, 2010. **274**(1): p. 11-20.

104. Al-Ali, K., S. Kodama, and H. Sekiguchi, *Modeling and simulation of methane dry reforming in direct-contact bubble reactor.* Solar energy, 2014. **102**: p. 45-55.

105. Ni, J., et al., *Carbon deposition on borated alumina supported nano-sized Ni catalysts for dry reforming of CH_4.* Nano Energy, 2012. **1**(5): p. 674-686.
106. Tomishige, K., et al., *Comparative study between fluidized bed and fixed bed reactors in methane reforming combined with methane combustion for the internal heat supply under pressurized condition.* Applied Catalysis A: General, 2002. **223**(1-2): p. 225-238.
107. Dahl, J.K., et al., *Dry reforming of methane using a solar-thermal aerosol flow reactor.* Industrial & Engineering Chemistry Research, 2004. **43**(18): p. 5489-5495.
108. Pereira, A.L.C., et al., *A comparison between the precipitation and impregnation methods for water gas shift catalysts.* Journal of Molecular Catalysis A: Chemical, 2008. **281**(1-2): p. 66-72.
109. Li, G., L. Hu, and J.M. Hill, *Comparison of reducibility and stability of alumina-supported Ni catalysts prepared by impregnation and co-precipitation.* Applied Catalysis A: General, 2006. **301**(1): p. 16-24.
110. de Jong, K.P., *Deposition precipitation.* Synthesis of solid catalysts, 2009: p. 111-134.
111. Perego, C. and P. Villa, *Catalyst preparation methods.* Catalysis Today, 1997. **34**(3-4): p. 281-305.
112. Deraz, N., *The comparative jurisprudence of catalysts preparation methods: I. Precipitation and impregnation methods.* J. Ind. Environ. Chem, 2018. **2**(1): p. 19-21.
113. Yang, G. and S.-J. Park, *Conventional and microwave hydrothermal synthesis and application of functional materials: A review.* Materials, 2019. **12**(7): p. 1177.
114. Volovych, I., *Sol-gel processes in catalysis.* 2014.
115. Naeem, M.A., et al., *Hydrogen production from methane dry reforming over nickel-based nanocatalysts using surfactant-assisted or polyol method.* International journal of hydrogen energy, 2014. **39**(30): p. 17009-17023.
116. Zhang, X., et al., *Carbon dioxide reforming of methane over Ni nanoparticles incorporated into mesoporous amorphous ZrO_2 matrix.* Fuel, 2015. **147**: p. 243-252.

CHAPTER 3: METHODOLOGY

3.1 Synthesis of Catalyst

The synthesis of $MgAl_2O_4$, TiO_2 nanoparticles was brought by hydrothermal method after which composite Co/$MgAl_2O_4$-TiO_2 was synthesized by impregnation method. Different cobalt loadings of 2.5%, 5% and 7.5% were used for the composite synthesis in order to study the effect of loading with the catalytic performance.

3.1.1 Synthesis of $MgAl_2O_4$ Nanoparticles

$MgAl_2O_4$ spinel was prepared by the coprecipitation followed hydrothermal method as shown by the detailed steps in Fig 3.1. To prepare $MgAl_2O_4$, Mg $(NO_3)_2 \cdot 6H_2O$ (99.99 %, Sigma Aldrich) and Al $(NO_3)_3 \cdot 9H_2O$ (98 %, Honeywell Fluka) were the initial salts used. The stoichiometric amount of salts were added in deionized water with continuous stirring and mixing to form homogeneous solution. To adjust the pH of the solution, precipitating agent of ammonia solution (32%) was used and added dropwise to maintain the pH in the range of 10-11.5 with milky white appearance of final solution. The solution was then transferred to hydrothermal autoclave and then treated in oven conditions of 200 °C for about 24 hrs and then left for overnight cooling. The resulting precipitate was then centrifuged and washed with deionized water and ethanol and the pH was brought to 7.0[1]. The slurry was then dried for overnight and then grinded to obtain the powder which is then calcined in furnance with conditions set at 800 °C for 5 h. The calcined sample was then grinded and collected in the form of fine $MgAl_2O_4$ particles.

3.1.2 Synthesis of TiO_2

TiO_2 synthesis followed the same steps as $MgAl_2O_4$ synthesis and was prepared by hydrothermal method. TiO_2 nanowires (NWs) were synthesized by Titanium (IV) oxide (99%, Sigma-Aldrich) nano powder as a starting material. 0.70 g of nano powder was added in 70 ml quantity of 10 M NaOH basic solution. The solution was homogenized by continuous stirring after which it is transferred to hydrothermal autoclave and oven treated with conditions set at 160 °C and 5 h. The solution was cooled and centrifuged to obtain white precipitates followed by washing with

deionized water and 0.1 M HCL solution[2]. The solution was then dried in oven at 100 °C to obtain the final product.

3.1.3 Synthesis of Co/$MgAl_2O_4$-TiO_2 Nanocomposite

Co/$MgAl_2O_4$-TiO_2 nanoparticles were prepared by the already prepared $MgAl_2O_4$ and TiO_2 NWs and Co $(NO_3)_2.6H_2O$ (98%, Merck) salt by the wetness impregnation method.

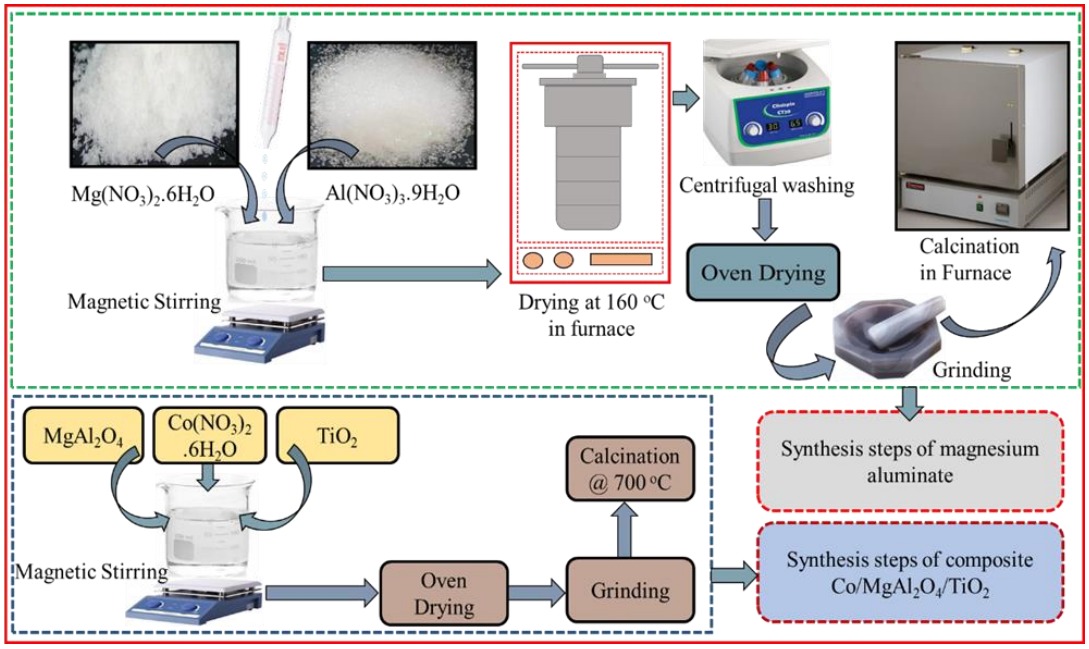

Fig 3.1 Step-wise synthesis of composite Co/$MgAl_2O_4$-TiO_2

The impregnation method started with the mixing of 1 g $MgAl_2O_4$ and 0.1 g TiO_2 NWs in 100ml deionized water and solution was allowed to mix for half an hour under constant stirring. After which 0.25 g Co $(NO_3)_2.6H_2O$ was added in the mixture with constant stirring conditions for 5 h at 70 °C. The resulted slurry was then dried in oven at 100 °C overnight and cooled followed by calcination in furnance at 750 °C for about 5 h. The sample was named as 5%Co/10% TiO_2 -$MgAl_2O_4$. Similar process was followed for the composite synthesis with 2.5% cobalt loading and 7.5% cobalt loading but the only difference is 0.125 g and 0.375 g Co $(NO_3)_2.6H_2O$ was added for 2.5% cobalt loading and 7.5% cobalt loaded composite respectively. The detailed schematic of the composite synthesis is shown in Fig 3.1.

3.2 Catalyst Characterizations

The prepared catalysts were then brought to testing using different characterisations which are explained in the below sections.

3.2.1 X-ray Diffraction (XRD)

To analyse the crystalline structure and phase transitions of the prepared samples, XRD was used. The calcined and well grinded samples were brought to Bruker D8 advanced X-ray diffractometer as shown in Fig 3.2 with specifications of 1.5418 Å irradiation wavelength at 40 kV and 40 mA set conditions to identify their diffraction peaks. Additionally diffraction angles range was set at 5°–90° and 0.05°-2θ step size was used to analyse XRD patterns. Also the size of crystallite was obtained using Scherrer equation[3].

Fig 3.2 Advanced X-ray Diffractometer

3.2.2 Scanning Electron Microscopy (SEM)

The morphology of the both fresh and spent samples were visualized by SEM. The SEM images were obtained using SEM Model JSM-6490A JEOL (Japan) as shown in Fig 3.3 and micro level images with different resolutions of 5 µm, 1 µm and 500 nm were obtained additionally with EDS images at 10 µm resolution. The microscope resolution was set at 3 nm and 30 kV operation parameter.

Fig 3.3 Scanning Electron Microscope

3.2.3 Thermogravimetric Analysis (TGA)

To observe the deposited carbon associated with fresh and spent samples and to seek their respective thermal stability and weight losses with respect to temperature changes, TGA was used. TGA analysis was performed using TGA 5500, TA Instruments (USA) as shown in Fig 3.4. 10mg sample was used for TGA analysis while the nitrogen flow was maintained at 25 mL min^{-1} and maximum temperature of 900 °C with 10 °C min^{-1} heating rate was used.

Fig 3.4 Thermogravimertric Analyser

3.2.4 Fourier Transform Infrared Spectroscopy (FTIR)

To check out the corresponding functional groups present in the sample, FTIR was used. FTIR analysis was done using Cary 630 FTIR (Agilent Technologies, USA) as shown in Fig 3.5 and wavenumber were set in the range 4000 cm^{-1} to 650 cm^{-1}.

Fig 3.5 Fourier Transform Infrared Spectroscopy

3.3 Experimental Setup

The setup provided with fixed bed reactor used for DRM reaction is shown in Fig 3.6.

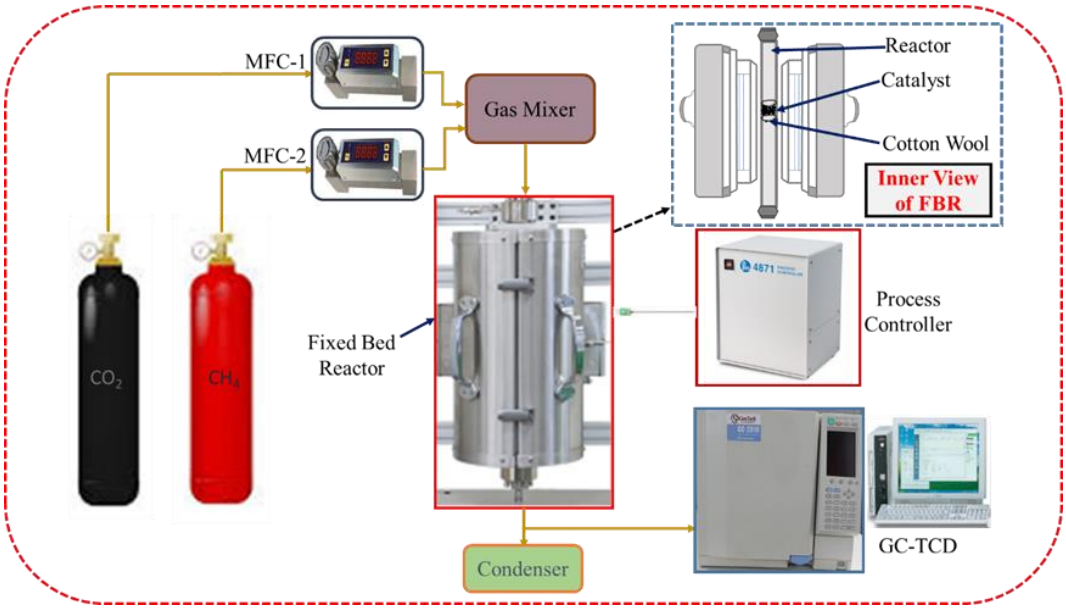

Fig 3.6 Experimental setup of DRM reaction

To carry out the process, fluidized bed reactor of PARR (Model # LSP-2.38-0-32-1C-2335EEE, Moline USA) was replaced with modified fixed bed reactor 2.5 ft. in length of SS 316 material tube with ½ inch dia. opening fixed with SS RED union on both ends and connected to gas mixer.

The system was connected with MF4600 series type digital mass flow controllers for feed gas supply. To control the temperature of the reactor, 4871 series process controller was used. Also to control catalyst bed temperature, thermocouple of K-type was used. The catalyst was handled in bed between the suspended glass wool and kept in the position in reactor by supports.

N_2 was used as a purging gas in the reactor and the flow was set for 20 mL min^{-1} with the reactor temperature set at 700 °C for 1 h before carrying out reaction. CH_4 (99.99%) and CO_2 (99.99%) were used as feed gases with flow rate of set at 10 $mlmin^{-1}$ while 0.5 g catalyst was used and the reaction temperature was 750 °C. The products were obtained after passing through condenser and brought to gas chromatograph (GC 2010 plus Shimadzu) equipped with thermal conductivity detector (TCD) for further gas analysis. GC operating conditions were set at 200 °C column temperature and 5 min retention time.

3.4 Catalytic Activity

To check out the catalyst activity and stability tests, following equations are used as written below in eqs. (10) to (15). These results include the conversions of the reactants, selectivity and yields of the reactants.

$$CH_4 \text{conversion}\left(X_{CH_4}\right)\% = \left[\frac{(n\,CH_4)_{converted}}{(n\,CH_4)_{feed}} \times 100\right] \tag{10}$$

$$CO_2 \text{ conversion}\left(X_{CO_2}\right)\% = \left[\frac{(nCO_2)_{converted}}{(nCO_2)_{feed}} \times 100\right] \tag{11}$$

$$CO \text{ selectivity}\left(S_{CO}\right)\% = \left[\frac{(nCO)_{produced}}{(nCH_4 + nCO_2)_{converted}} \times 100\right] \tag{12}$$

$$H_2 \text{ selectivity}\left(S_{H_2}\right)\% = \left[\frac{(nH_2)_{produced}}{(2 \times nCH_4)_{converted}} \times 100\right] \tag{13}$$

$$H_2 \text{ yield}\left(Y_{H_2}\right)\% = \left[\frac{(nH_2)_{produced}}{2 \times (nCH_4)_{feed}} \times 100\right] \tag{14}$$

$$CO \text{ yield}\left(Y_{CO}\right)\% = \left[\frac{(nCO)_{produced}}{(nCH_4 + nCO_2)_{feed}} \times 100\right] \tag{15}$$

References

1. Khoja, A.H., M. Tahir, and N.A. Saidina Amin, *Evaluating the performance of a Ni catalyst supported on La_2O_3-$MgAl_2O_4$ for dry reforming of methane in a packed bed dielectric barrier discharge plasma reactor*. Energy & Fuels, 2019. **33**(11): p. 11630-11647.
2. Nor, A.M., et al., *Synthesis of TiO_2 nanowires via hydrothermal method.* Japanese Journal of Applied Physics, 2012. **51**(6S): p. 06FG08.
3. Charisiou, N., et al., *Syngas production via the biogas dry reforming reaction over nickel supported on modified with CeO_2 and/or La_2O_3 alumina catalysts.* Journal of Natural Gas Science and Engineering, 2016. **31**: p. 164-183.

CHAPTER 4: RESULTS AND DISCUSSION

4.1 Characterisations of Fresh Catalyst

The prepared fresh catalyst was characterized using various characterisations like XRD, SEM, TGA and FTIR in order to identify structures of constituents present in catalyst, its morphology, its behaviour with temperature change effect and to figure out the type of functional groups associated with catalyst.

4.1.1 XRD of Fresh Catalyst

XRD analysis was done to find out the crystalline phases within prepared catalyst as shown in Fig 4.1 with the associated details given in Table 4.1.

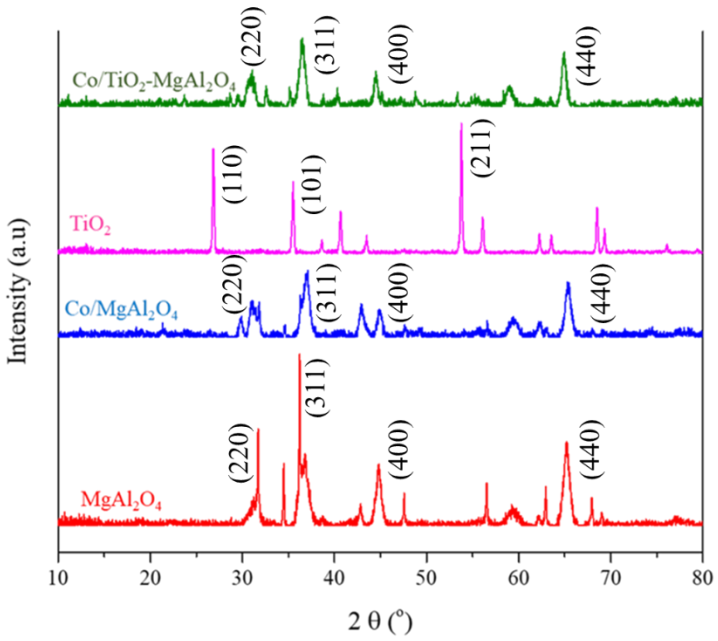

Fig 4.1 XRD of prepared fresh samples of $MgAl_2O_4$, $Co/MgAl_2O_4$, TiO_2, Co/TiO_2-$MgAl_2O_4$

The spinel $MgAl_2O_4$ (PDF# 21-1152) diffraction peaks were centred at $2\theta = 19.02°$ (hkl; 111), 31.27° (hkl; 220), 36.85° (hkl; 311), 44.8° (hkl; 400) and 65.2° (440) with

d-spacing of 0.466, 0.28, 0.243, 0.202 and 0.14nm respectively while the most intensified peak was observed at 36.85°[1, 2]. In the same way XRD of TiO_2 (PDF#21-1276) shown diffraction peaks at 2θ= 27.44° (hkl; 110), 36.08° (hkl; 101), 41.22° (hkl; 111), 54.32° (hkl; 211), 56.64° (220) and 69.0° (hkl; 301) with d-spacing of 0.32, 0.24, 0.218, 0.16, 0.162 and 1.35 nm respectively with the major peak at 54.32° while the rutile phase of tetragonal TiO_2 geometry was identified[3].

Table 4.1 XRD analysis of fresh catalyst

Sample Catalysts	**Compounds**	**Structure**	**PDF #**	**2θ (°)**	**Phase (hkl)**
$MgAl_2O_4$	-	Spinel	21-1152	36.85	311
$Co/MgAl_2O_4$	$MgAl_2O_4$	Spinel	21-1152	36.85	311
	$CoAl_2O_4$	Cubic	44-0160	44.63	400
	Co_3O_4	Cubic	43-1003	31.2	220
TiO_2	-	Tetragonal	21-1276	54.32	211
Composite(Co/TiO_2-$MgAl_2O_4$)	$MgAl_2O_4$	Spinel	21-1152	36.85	311
	$CoAl_2O_4$	Cubic	44-0160	44.63	400
	Co_3O_4	Cubic	43-1003	31.2	220
	TiO_2	Tetragonal	21-1276	54.32	211
	$CoTiO_3$	Hexagonal	15-0866	32.8	104

The XRD analysis of $Co/MgAl_2O_4$ shown three associated groups with diffraction peaks found were $MgAl_2O_4$, $CoAl_2O_4$ and Co_3O_4. $MgAl_2O_4$ was found to have same PDF#21-1152 and same diffraction peaks with same characteristics as discussed above while $CoAl_2O_4$ (PDF#44-0160) shown cubic structure with space group of Fd3m (227) and the diffraction peaks centred at 2θ= 31.74° (hkl; 220), 36.7° (hkl; 311) and 44.63° (hkl; 400) with d-spacing of 0.284, 0.244 and 0.20 nm respectively[4]. Similarly Co_3O_4 (PDF# 43-1003) shown cubic structure having space group Fd3m (227) with

diffraction peaks at 2θ= 31.2° (hkl; 220) and 36.8° (hkl; 311) with d-spacing 0.28 and 0.243 nm respectively[5].

The XRD analysis of composite Co/TiO_2-$MgAl_2O_4$ shown above discussed all the compounds with same diffraction peaks having same characteristics along with the presence of CoTiO3 (PDF# 15-0866) having hexagonal structure and space group R-3(148) while its diffraction peak was centred at 2θ= 32.8° (hkl; 104) and d-spacing 0.27 nm[6].

4.1.2 SEM/EDS of Fresh Catalyst

The morphology of the fresh prepared catalysts was captured by the SEM images of $MgAl_2O_4$, TiO_2, Co/TiO_2-$MgAl_2O_4$ as shown in Fig. 4.2 (a-f) with the resolutions of 5 μm and 1 μm. The morphology of $MgAl_2O_4$ depicted the blocked shaped spinel structure with sintering owing to high temperature calcination. The SEM image of TiO_2 shown the particles formation in fine form with some nanowires of TiO_2 present along with particles while the morphology of composite shown the presence of all the constituents within it by confirming the presence of $MgAl_2O_4$ spinel structure found along with the visuals of TiO_2 nanoparticles and nanowires in depth. The EDS of the prepared catalysts as shown in Fig. 4.3 (a-c) confirmed the presence of all the constituents within composite as EDS of $MgAl_2O_4$ shown Mg and Al peaks which are intensified while TiO_2 EDS results also shown presence of Ti and O species with some impurities found in it which got in process of preparation. Similarly the EDS image of composite also confirmed the presence of Co, Ti, O, Mg and Al constituents as verified by the peaks however some impurities were also present along with the sample.

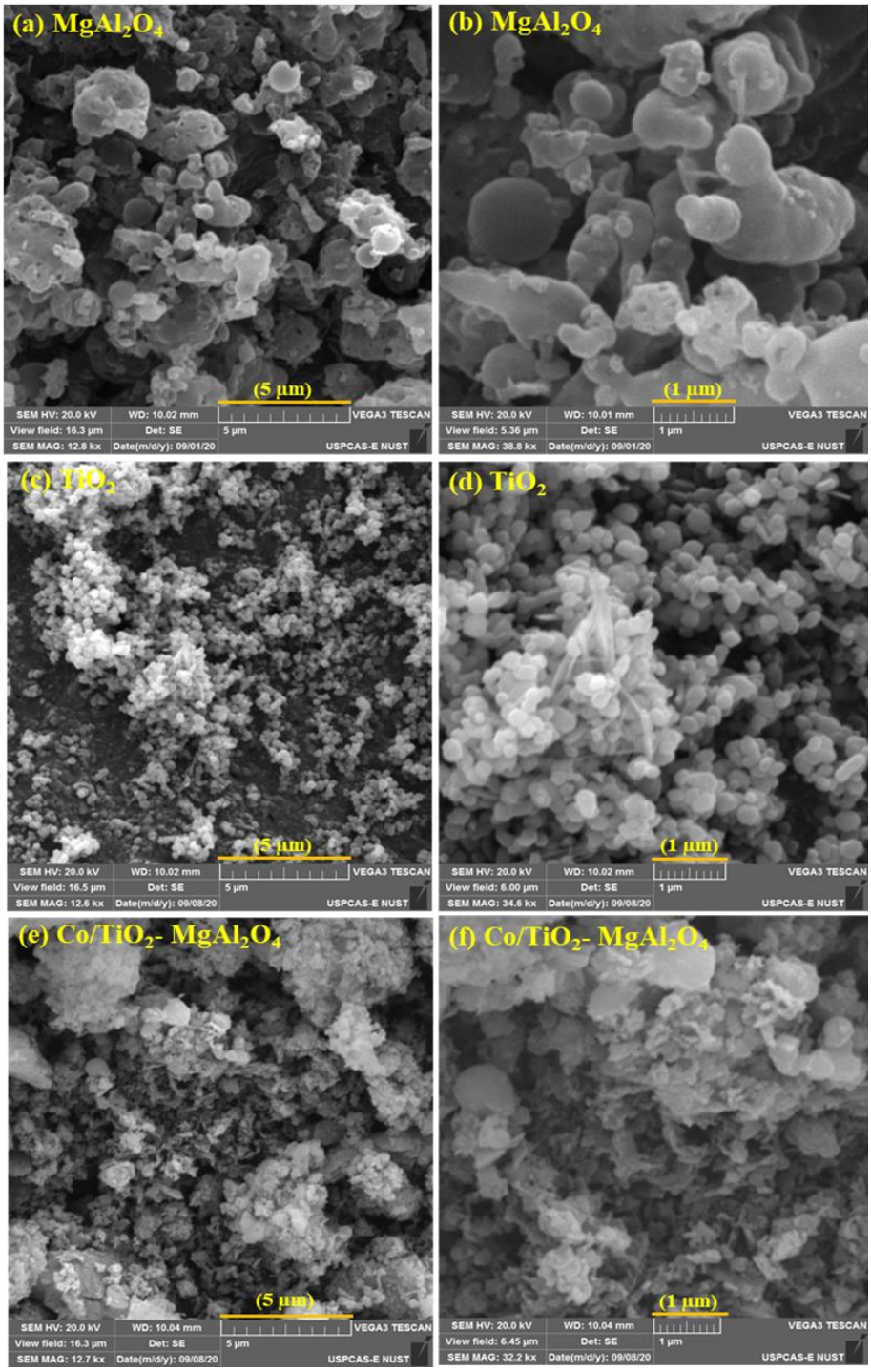

Fig 4.2 SEM images of prepared fresh samples (a-b) $MgAl_2O_4$; 5 µm and 1 µm (c-d) TiO_2; 5 µm and 1 µm (e-f) Co/TiO_2-$MgAl_2O_4$; 5 µm and 1 µm

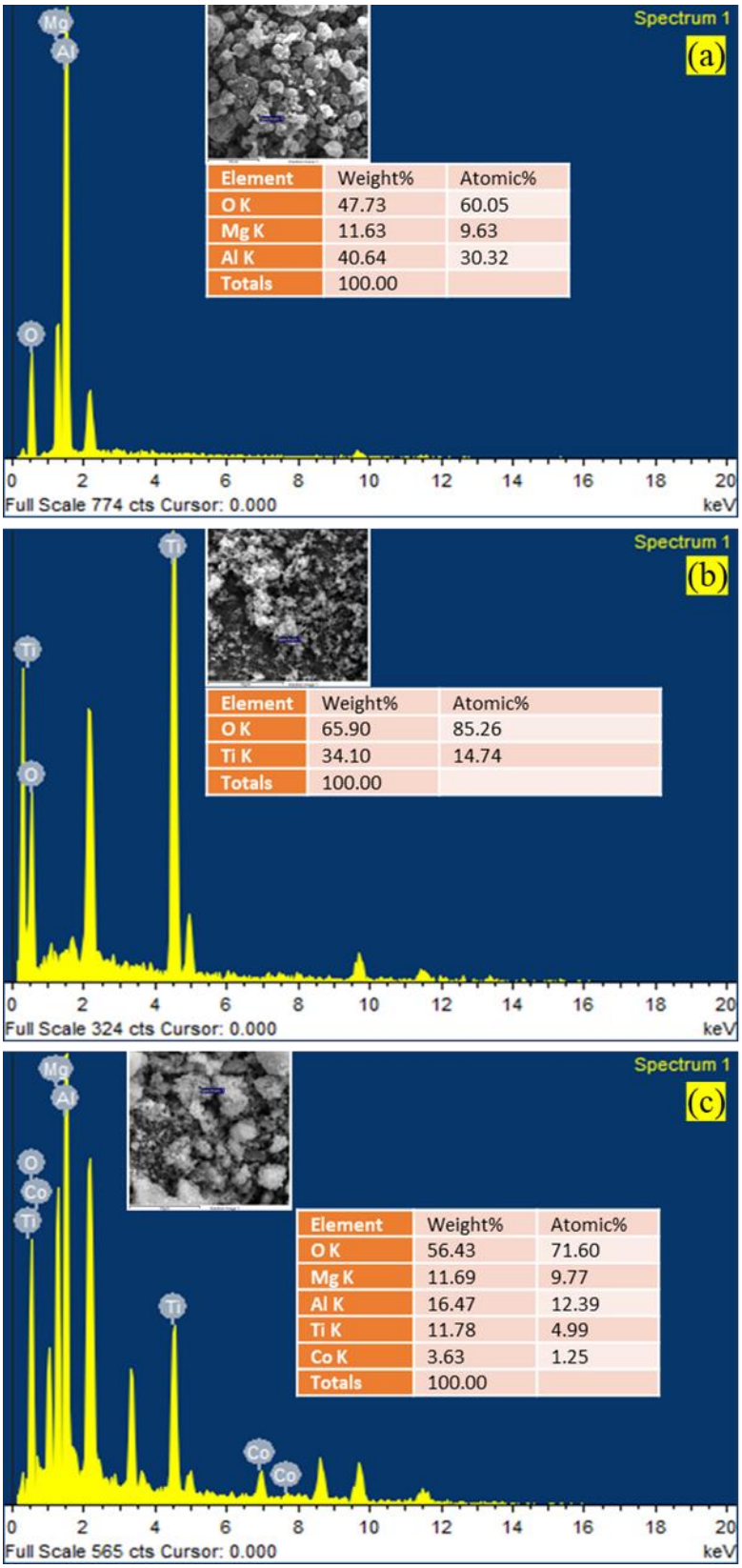

Fig 4.3 EDS of prepared fresh samples at 10 µm (a) $MgAl_2O_4$ (b) TiO_2 (c) Co/TiO_2-$MgAl_2O_4$

4.1.3 TGA of Fresh Catalyst

The thermal stability of the fresh prepared catalysts gone under investigation by the temperature change effect on weight losses of samples as shown in Fig. 4.4. The TGA curve for $MgAl_2O_4$ shown total weight loss of about 5% in which initial 3.5% of weight loss upto 150 °C was observed because of moisture removal and combustion of left unburnt nitrates while the rest of weight loss was due to conversions of hydroxide to oxides. The stability of TiO_2 was shown by TGA curve of TiO_2 which indicated total of 2% weight loss attributed to moisture removal and organic compounds decomposition.

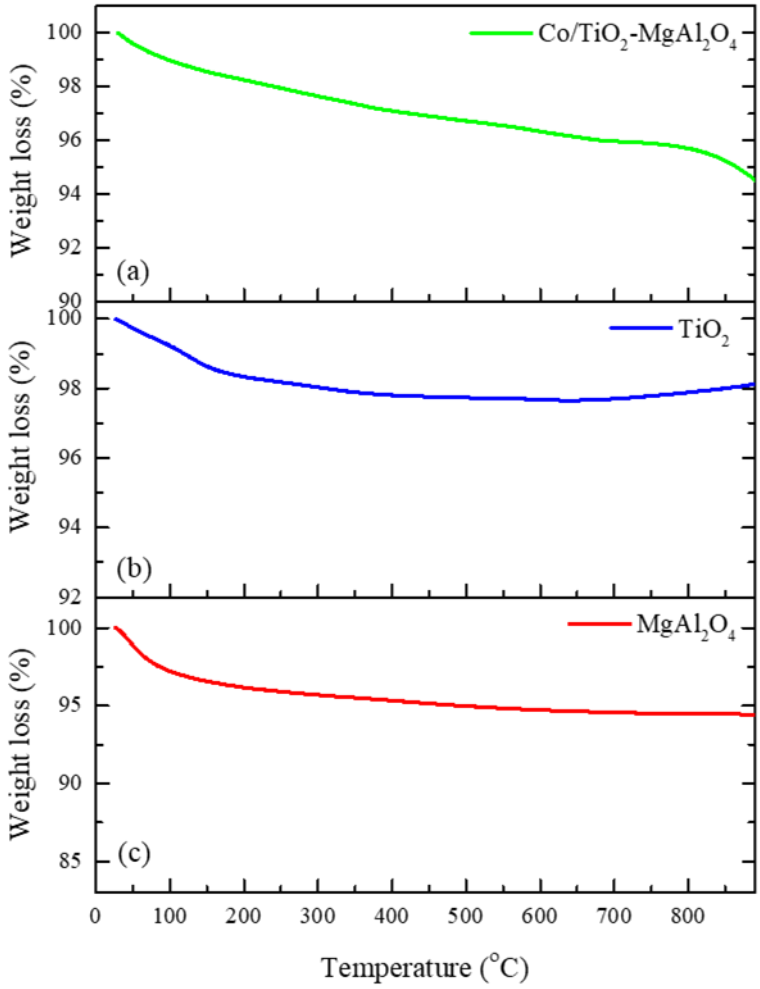

Fig 4.4 TGA of prepared fresh samples (a) $MgAl_2O_4$ (b) TiO_2 (c) Co/TiO_2-$MgAl_2O_4$

The weight gain was observed at high temperature for TiO_2 which was due to occurrence of oxidation processes within it. Similarly the 5% weight loss was observed

in composite TGA with gradual decrease in which initial loss was due to adsorbed moisture removal while the remaining was due to breakage of bonds and formation of intermediates within composite.

4.1.4 FTIR of Fresh Catalyst

FTIR identifies the functional groups and the bonds present in the samples. The FTIR of $MgAl_2O_4$, TiO_2, and Co/TiO_2-$MgAl_2O_4$ is shown in Fig. 4.5. FTIR of $MgAl_2O_4$ show peak at wave number close to 900 cm^{-1} while the stretching vibration of Al-O bonds fall in range of 700-900 cm^{-1} also M-O-M (M=Mg^{2+} & Al^{3+}) stretching vibration fall in range of 400-900 cm^{-1} which indicated the formation of spinel $MgAl_2O_4$[7-9]. Similarly the peak for TiO_2 was observed close to wavenumber 700 cm^{-1} which corresponds to Ti-O bonding confirming formation of TiO_2[10-12]. The composite shows peaks at 900 cm^{-1} corresponding to Mg-O-Al bonding, 744 cm^{-1} corresponding to Ti-O-Ti bonding and there was found also a small peak at wavenumber

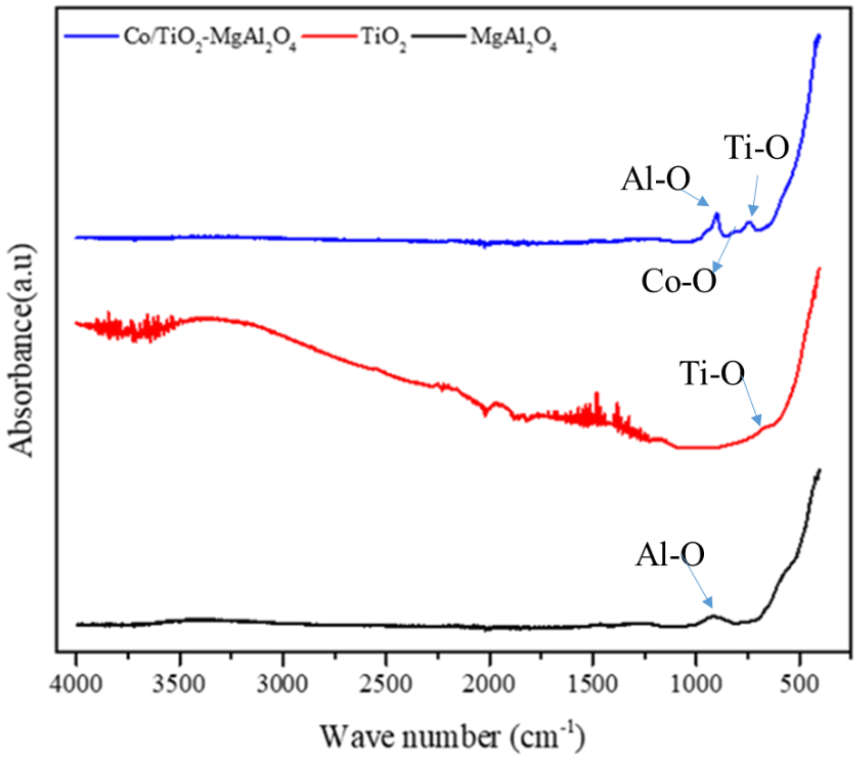

Fig 4.5 FTIR of the prepared fresh samples

around 850 cm^{-1} which shown the presence of O-Co-O bonding confirming Co_3O_4 formation[13]. The O-Co-O bond, O-Ti-O bond and Ti-O bond interact to form the $CoTiO_3$ specie as described in the stability results below. This specie contribute towards the catalyst overall stability by reacting with the C species produced during reaction.

4.2 Characterisation of Spent $Co/MgAl_2O_4$-TiO_2 Catalyst

The fresh composite was processed for 75 h in the reactor for the DRM reaction after which the spent composite was collected carefully and further characterised by XRD, SEM/EDX and TGA to find out the carbon formed over catalyst. The spent characterisations so done have been presented in Fig.4.6 and Fig.4.7. The XRD analysis of the spent catalyst revealed the existence

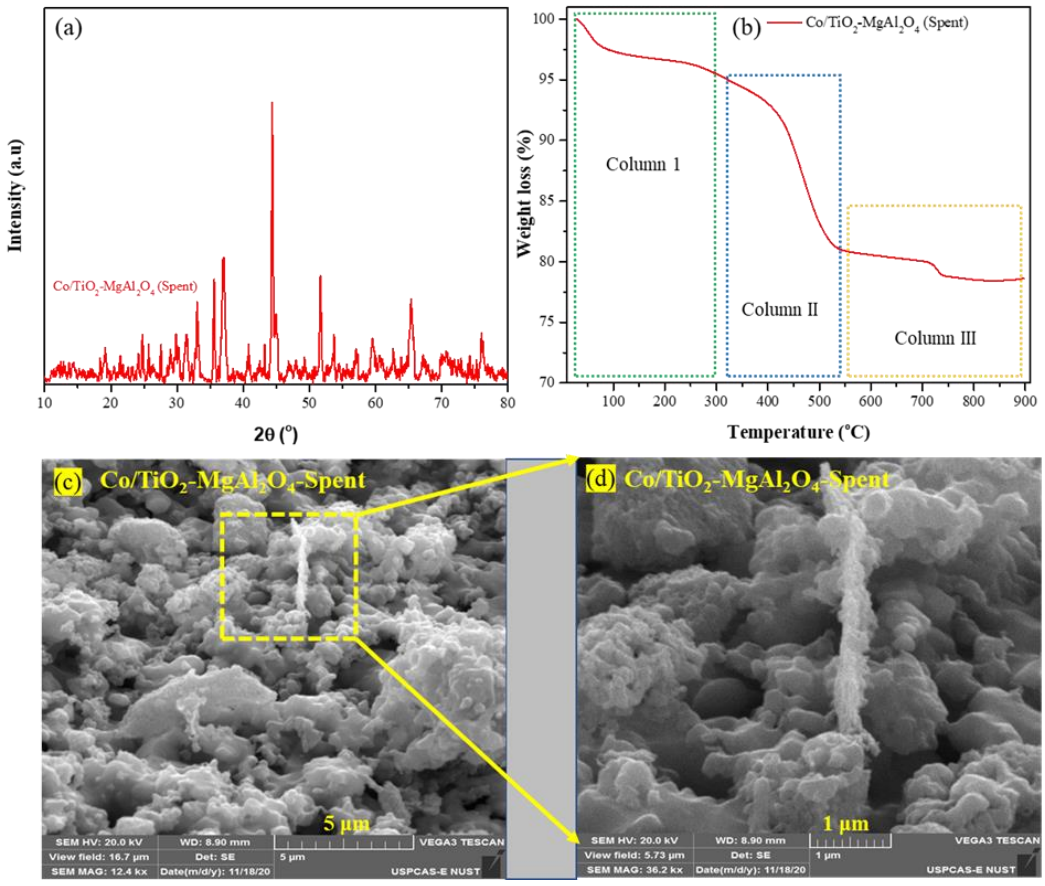

Fig 4.6 (a) XRD of spent Co/TiO_2-$MgAl_2O_4$ (b) TGA of spent Co/TiO_2-$MgAl_2O_4$ (c-d) SEM images of spent Co/TiO_2-$MgAl_2O_4$; 5 µm and 1 µm

of spinel $MgAl_2O_4$, TiO_2, $CoAl_2O_4$, Co_3O_4 and $CoTiO_3$ with same crystalline phases as found in the fresh composite XRD analysis. $MgAl_2O_4$ (PDF#21-1152) was found with same diffraction peaks with its main peak was centred at 36.85° (hkl; 311). TiO_2 (PDF#21-1276) found slight shift in peak centred at 51.8° (hkl; 211) with same rutile phase and tetragonal geometry. Also peak of $CoAl_2O_4$ (PDF#44-0160) slightly shifted at 36.0° (hkl; 311) however peaks of Co_3O_4 (PDF#43-1003) found peaks with same diffraction angles and characteristics as found in fresh sample. The diffraction peak of $CoTiO_3$ (PDF#15-0866) was centred at 32.8° (hkl; 104). The additional diffraction peak of graphite carbon (PDF#41-1487) was observed at 26.3° (hkl; 002) with hexagonal geometry and 0.337 nm d-spacing[14].

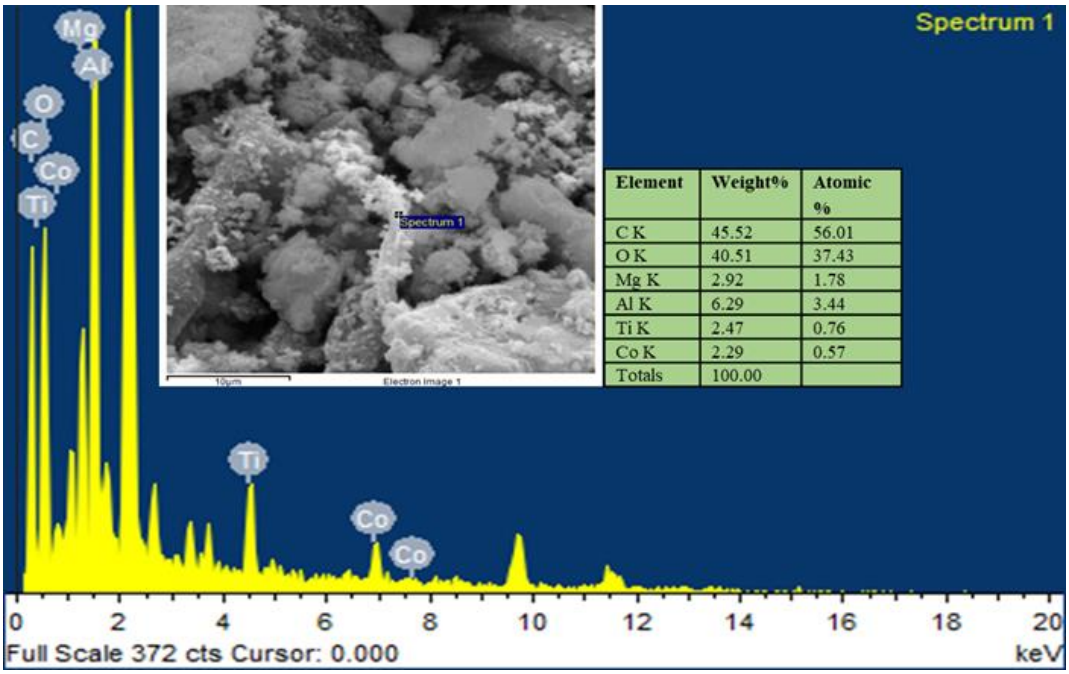

Fig 4.7 EDS image of spent Co/TiO_2-$MgAl_2O_4$

The TGA profile of spent catalyst got divided into three columns with temperature change. The first column shown the removal of adsorbed moisture and volatile compounds up to 300 °C with total of 4-5% weight loss[15]. The second column weight loss was observed due to α-C and β-C species found in the spent catalyst and significant weight loss of 14% was associated with it from 300 °C to 500 °C[16]. The weight loss at higher temperature was attributed to filamentous carbon (γ-C) which was found to be in lower amount contributing 2-3% in weight loss[17].

The SEM and EDS results confirmed that catalyst surface was covered with carbon as shown in Fig.4.6 (c-d) and Fig.4.7. The total amount of carbon so found was as much as 45% in spent catalyst which include the different forms of carbon species formation during reaction but the catalytic activity and stability results with high activity indicated the presence of more non-deactivating type graphitic carbon species formed which resulted because of decomposition of methane at higher temperature[18].

4.3 Catalyst Activity and Stability Tests

A series of activity tests were conducted by varying the operational parameters like reactor temperature, feed flow rate and also the feed gas ratio to optimize the results. The catalysts were tested for the reactor temperature of 700 °C, 750 °C, 800 °C and 850 °C and the activity results shown improvement with the increase in the temperature with the relatively good activity results at 750 °C. The feed flow rate was also varied from 80 mL min^{-1} to 20 mL min^{-1} in equal proportion in order to analyse the results however the better results were obtained at 20 mL min^{-1} feed flow rate owing to more contact time. A couple of tests were conducted at different feed gas ratios in order to check the effect of the individual feed gases on the final product. However the best results came with the use of unity proportion feed gases ratio giving the syngas in the product close to unity. The catalysts so prepared were introduced into the fixed bed reactor for the DRM reaction to check out the catalytic activity and stability results with the conditions of reactor temperature at 750 °C, catalyst loading of 0.5 g, total feed flow rate set at 20 mL min^{-1} and the feed gas ratio of 1.

4.3.1 Activity Tests of Individual Supports, Metal-Support and Composite

The conversions of CH_4 and CO_2 are presented in Fig.4.8 while the selectivity and yield of CO and H_2 are presented in Fig.4.9 and Fig.4.10 respectively with 5 h TOS over individual supports, metal-supports interaction and the final composite. These results shown the supports effect, then effect of metal-supports and final combination of supports and metal to form composite effect over activity results.

The TiO_2 support alone doesn't give satisfying activity results as shown by the associated lower CH_4 and CO_2 conversions with lower H_2 and CO selectivity and yield results. However TiO_2 shown good metal support interaction when interacted with metal but in this case interaction of Co with TiO_2 shown lower activity results with

lower conversions of methane and carbon dioxide and lower selectivity and yield of hydrogen and carbon monoxide[19]. The reason was due to the formation of oxidation induced $CoTiO_3$ which caused deactivation.

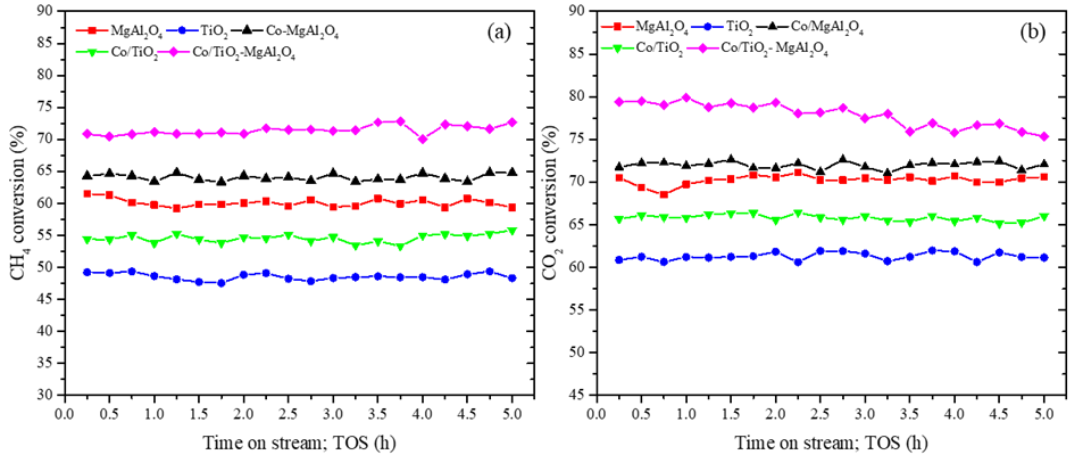

Fig 4.8 TOS effect vs (a) CH_4 conversion (b) CO_2 conversion for different fresh samples; catalyst loading = 0.5 g, reaction temperature = 750 °C, feed ratio (CO_2/CH_4) = 1, feed flow rate = 20 mL min^{-1}

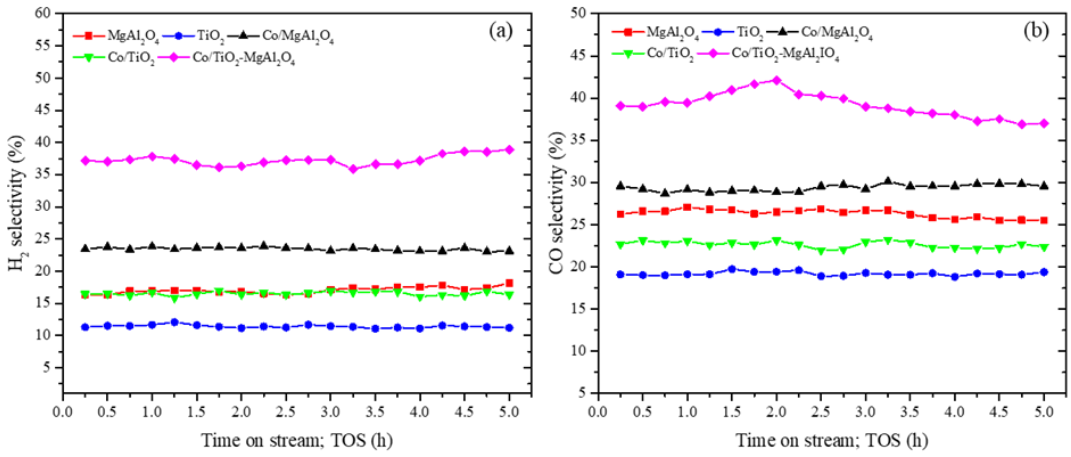

Fig 4.9 TOS effect vs (a) H_2 Selectivity (S_{H2}) (b) CO selectivity (S_{CO}) for different fresh samples; catalyst loading = 0.5 g, reaction temperature = 750 °C, feed ratio (CO_2/CH_4) = 1, feed flow rate = 20 mL min^{-1}

The $MgAl_2O_4$ support when used alone for the activity results shown good results with conversion of CH_4 as high as 61% and 70% CO_2 because $MgAl_2O_4$ is an excellent support and provides both acidic and basic active sites and exhibited good thermal stability[20]. The acidic portion of support played role in methane decomposition

while the carbon dioxide dissociation was resulted because of basic support[21]. The interaction of $MgAl_2O_4$ support with Co however shown intermediate results for CH_4 and CO_2 conversions of 65% and 72% respectively which was mainly due to formation of $CoAl_2O_4$ compound which resulted in relatively lower activity however contributing towards carbon deposition inhibition.

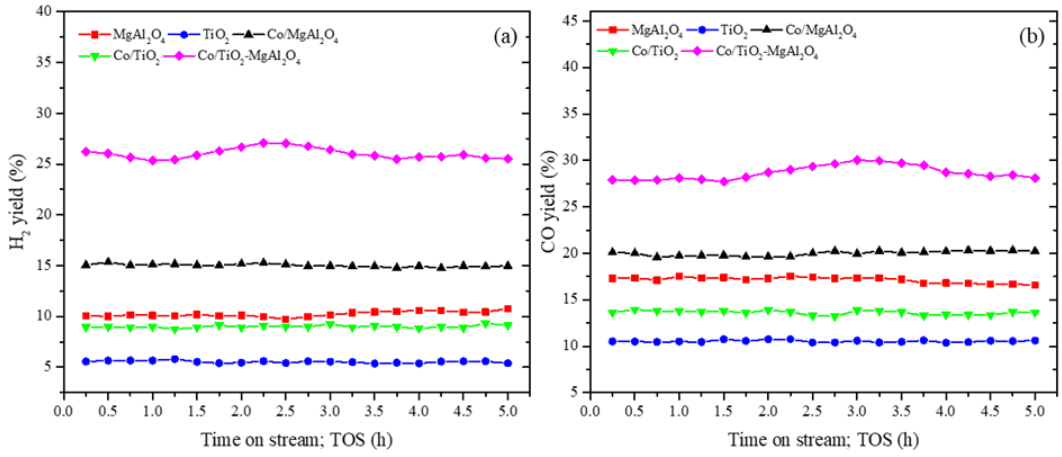

Fig 4.10 TOS effect vs (a) H_2 Yield (Y_{H2}) (b) CO Yield (Y_{CO}) for different fresh samples; catalyst loading = 0.5 g, reaction temperature = 750 °C, feed ratio (CO_2/CH_4) = 1, feed flow rate = 20 mL min^{-1}

The activity results of composite Co/TiO_2-$MgAl_2O_4$ shown the maximum CH_4 and CO_2 conversions of 72% and 80% respectively and the average 38% selectivity of H_2 and 40% selectivity for CO while the yield results shown 28% average H_2 yield and 30% CO yield. The higher activity results were due to the bi-supports interaction with metal providing active sites in bulk number and good interaction of metal and supports providing higher stability.

4.3.2 Screening Test of Composite with Different Cobalt Loadings

The screening tests were conducted for the $MgAl_2O_4$ support and the composites with different cobalt loading as shown in Fig.4.11. The overall results shown comparatively higher CO_2 conversions compared to CH_4 conversions which is the additional reaction of CO_2 with carbon resulted from methane decomposition[22]. For $MgAl_2O_4$, X_{CH4} and X_{CO2} were 61% and 68.5% respectively while S_{H2} and S_{CO} were 17.5% and 26.5% and similarly Y_{H2} and Y_{CO} of 11% and 17% respectively were recorded. For the

composite with different cobalt loadings, the increasing trend of conversions, selectivity and yield was resulted with the increase of cobalt loading.

For CH_4 and CO_2 conversions, 2.5% cobalt loaded composite shown 68% X_{CH4} and 73% X_{CO2} and it increased with cobalt loading with the highest recorded for 7.5% cobalt loaded composite having 76% X_{CH4} and 83% X_{CO2}. Similarly 2.5% cobalt loaded composite shown S_{H2} and S_{CO} of 26% and 31% respectively while remained highest with 43% S_{H2} and 46.5% S_{CO} for 7.5% cobalt

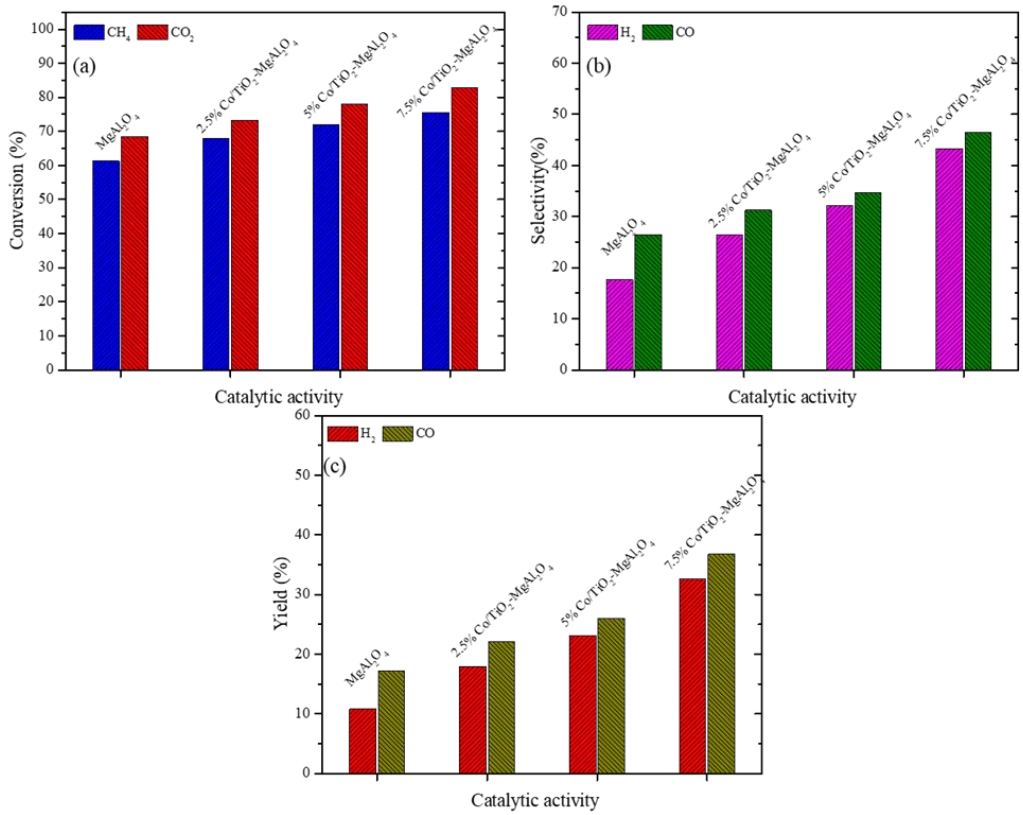

Fig 4.11 Effect of cobalt loading over $TiO_2/MgAl_2O_4$ (a) conversion (X_{CH4} and X_{CO2}) (b) Selectivity (S_{H2} and S_{CO}) (c) Yield (Y_{H2} and Y_{CO}); catalyst loading = 0.5 g, reaction temperature = 750 ˚C, feed ratio CO_2/CH_4 = 1, feed flow rate = 20 $mLmin^{-1}$

loaded composite. Similarly the 2.5% cobalt loaded composite shown 18% and 22% yield of H_2 and CO respectively and the yield also increased with cobalt loading increment with highest for 7.5% cobalt loaded composite having 33% Y_{H2} and 37% Y_{CO}.

For the composite with 2.5% cobalt loading the comparatively lower activity results were due to lower available active sites as fast CO_2 activation produced more oxygen species resulted in oxidation of active sites of Co and formation of more inactive species on Co[23]. The higher cobalt loading of 7.5% shown higher activity results but the carbon deposition is the problem associated with higher carbon loading which seemed to be sorted out by the oxygen species provided in excess by CO_2 dissociation which react with carbon species from methane decomposition resulting in CO formation and the activity remained higher[24]. However high cobalt loaded sample suffer stability issues and get deactivate with time.

4.3.3 Stability Test of Composite

The stability results for the composite were investigated where the stability results for conversion and selectivity over 75 h time of stream effect has been shown in Fig.4.12 while the stability results for yield and syngas ratio over 75 h TOS effect has been shown in Fig.4.13. The stability tests were conducted for 5% Co/TiO_2-$MgAl_2O_4$ and the results shown the increase in CO_2 followed by decrease in conversion till stability however conversion remains between 70 to 80%. The CH_4 conversion increased gradually from 55% to 70% for the first 30 h and then roamed between 60% and 70% for rest of time.

The selectivity and yield results shown the same trend with the gradual increase in selectivity and yield for first 55 h and then slightly decrease over the remaining time of operation. H_2/CO ratio was 0.9 on average over 75 h TOS. The reason for higher CO produced were the comparative fast CO_2 dissociation and its reaction with surface carbon along with reaction of $CoTiO_3$ specie with carbon. Also possibly H_2O off the RWGS reaction reacted with carbon to produce more amount of H_2 and CO.

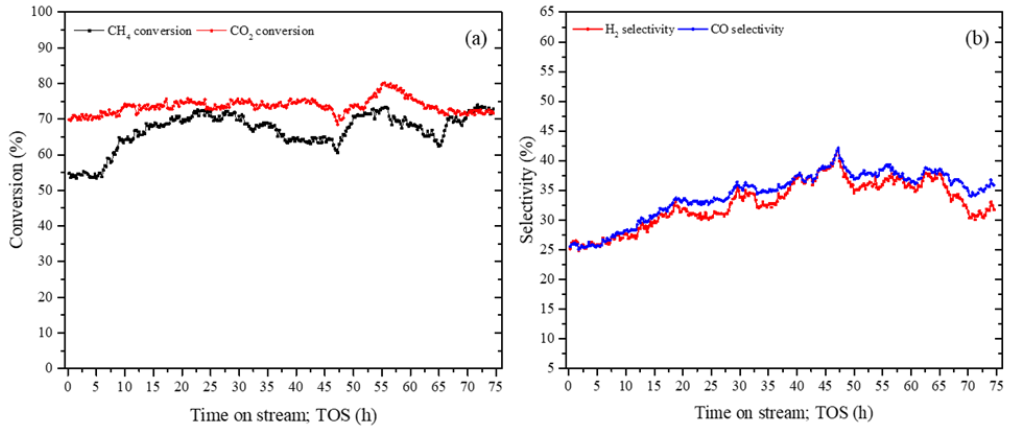

Fig 4.12 TOS effect vs (a) conversion (X_{CH4} and X_{CO2}) (b) Selectivity (S_{H2} and S_{CO}) over 5% Co/TiO_2-$MgAl_2O_4$; catalyst loading = 0.5 g, reaction temperature = 750 °C, feed ratio (CO_2/CH_4) = 1, feed flow rate = 20 mL min^{-1}

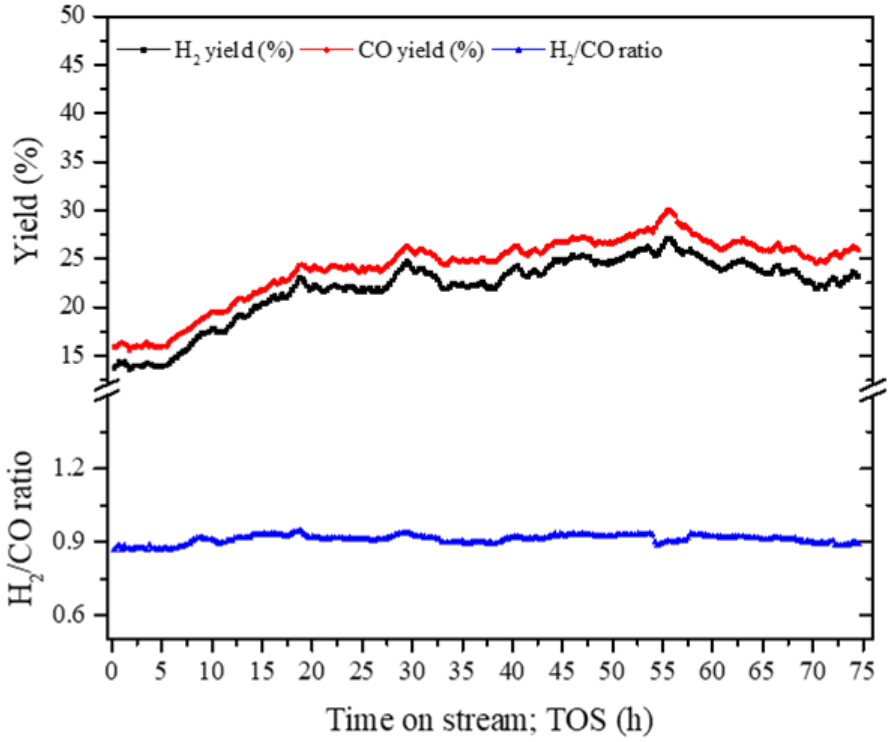

Fig 4.13 TOS effect vs Yield (Y_{H2} and Y_{CO}) and H_2/CO ratio over 5% Co/TiO_2-$MgAl_2O_4$; catalyst loading = 0.5 g, reaction temperature = 750 °C, feed ratio (CO_2/CH_4) = 1, feed flow rate = 20 mL min^{-1}

4.4 Reaction Mechanism

The possible reactions occurring during reaction are given in eq. (16) to eq. (19) and reaction mechanism is shown in Fig.4.14. The reaction initiated with the adsorption of CH_4 on cobalt and resulted in carbon and hydrogen species as shown in eq.(16) after which the hydrogen gas is produced as shown by eq.(17)[25, 26]. The cobalt species interacted with supports TiO_2 and $MgAl_2O_4$ along with dissociation of CO_2 to form CO as shown in eq. (18) while the inactive $CoTiO_3$ so produced reacted with carbon to produce CO as shown in eq. (19).

$$CH_4 + 2Co \rightarrow C\text{-}Co + H\text{-}Co \quad (16)$$

$$2H\text{-}Co \rightarrow H_2 + 2Co \quad (17)$$

$$2Co + CO_2 + TiO_2 + MgAl_2O_4 \rightarrow CoMgAl_2O_4 + CoTiO_3 + CO \quad (18)$$

$$C\text{-}Co + CoTiO_3 \rightarrow 2Co + TiO_2 + CO \quad (19)$$

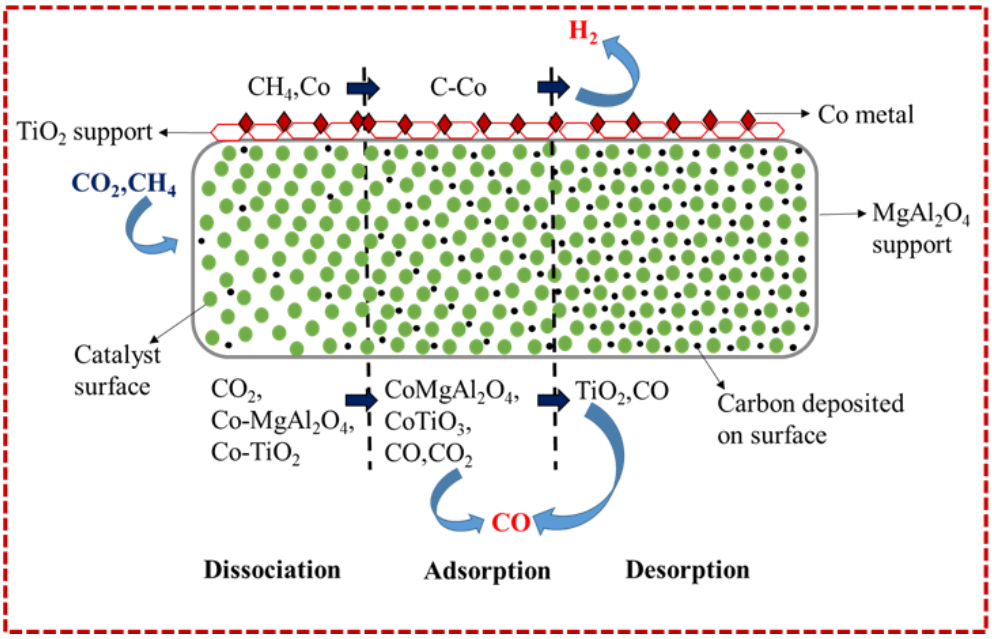

Fig 4.14 Reaction Mechanism of Co/TiO_2-$MgAl_2O_4$ for DRM reaction

Summary

The fresh prepared composite Co/TiO_2-$MgAl_2O_4$ was characterised by XRD, SEM, TGA and FTIR analysis. XRD results of composite shown all associated groups of $MgAl_2O_4$, TiO_2, Co_3O_4, $CoAl_2O_4$ and $CoTiO_3$ with different diffraction peaks and

different structures. SEM results of composite shown the presence of all constituents having block shaped $MgAl_2O_4$ spinel with TiO_2 nanowires in depth. TGA results of composite shown slight loss in weight owing to moisture removal, bonds breaking and intermediates formation while the FTIR results shown the Mg-O-Al, Ti-O-Ti and O-Co-O bondings corresponding to respective wavenumbers and peaks for the composite. The spent catalyst obtained after activity tests were characterised and the spent XRD shown additional graphitic carbon peaks observed while the SEM and TGA results also indicated the formation of carbon after 75 h activity tests.

The activity tests were conducted for individual supports, their combination and composite and the results shown higher conversions of CH_4 and CO_2 with 72% and 80% respective values, higher selectivity and yield results of H_2 and CO for the Co/TiO_2-$MgAl_2O_4$ composite. The Co loading effect was studied using 2.5%, 5% and 7.5% Co loading for the composite and the results indicated the increase in the activity results with increase in loading however for stability results 5% Co loaded composite shown higher stability of 75 h with the H_2/CO ratio of 0.9.

References

1. Saberi, A., et al., *Development of $MgAl_2O_4$ spinel coating on graphite surface to improve its water-wettability and oxidation resistance.* Ceramics international, 2009. **35**(1): p. 457-461.
2. Jiao, Y., et al., *Synthesis of a High-Stability Nanosized Pt-Loaded $MgAl_2O_4$ Catalyst for n-Decane Cracking with Enhanced Activity and Durability.* Industrial & Engineering Chemistry Research, 2020. **59**(10): p. 4338-4347.
3. Maruthapandi, M., et al., *Sonochemical preparation of polyaniline@ TiO_2 and polyaniline@ SiO_2 for the removal of anionic and cationic dyes.* Ultrasonics Sonochemistry, 2020. **62**: p. 104864.
4. Wang, Y., et al., *Irradiation synthesis and characterization of $CoAl_2O_4$: Ce and Mn-codoped $CoAl_2O_4$: Ce phosphors.* Optik, 2020: p. 164508.
5. Zhou, Y., et al., *Controlled synthesis and characterization of hybrid Sn-doped Co_3O_4 nanowires for supercapacitors.* Materials Letters, 2018. **216**: p. 248-251.

6. Wang, Q., et al., *The flux growth of single-crystalline $CoTiO_3$ polyhedral particles and improved visible-light photocatalytic activity of heterostructured $CoTiO_3/gC_3N_4$ composites.* Dalton Transactions, 2016. **45**(44): p. 17748-17758.
7. Thanabodeekij, N., et al., *Correlation of sol–gel processing parameters with microstructure and properties of a ceramic product.* Materials characterization, 2003. **50**(4-5): p. 325-337.
8. Adak, A., S. Saha, and P. Pramanik, *Synthesis and characterization of $MgAl_2O_4$ spinel by PVA evaporation technique.* Journal of materials science letters, 1997. **16**(3): p. 234-235.
9. Sanjabi, S. and A. Obeydavi, *Synthesis and characterization of nanocrystalline $MgAl_2O_4$ spinel via modified sol–gel method.* Journal of Alloys and Compounds, 2015. **645**: p. 535-540.
10. Tai, J.Y., et al., *Dopant-free oxygen-rich titanium dioxide: LED light-induced photocatalysis and mechanism insight.* Journal of Materials Science, 2017. **52**(19): p. 11630-11642.
11. Etacheri, V., et al., *Oxygen rich titania: A dopant free, high temperature stable, and visible-light active anatase photocatalyst.* Advanced Functional Materials, 2011. **21**(19): p. 3744-3752.
12. Sim, L.C., et al., *Mechanistic characteristics of surface modified organic semiconductor g-C_3N_4 nanotubes alloyed with titania.* Materials, 2017. **10**(1): p. 28.
13. Prabaharan, D.D.M., et al., *Precipitation method and characterization of cobalt oxide nanoparticles.* Applied Physics A, 2017. **123**(4): p. 264.
14. Guler, M., T. Dogu, and D. Varisli, *Hydrogen production over molybdenum loaded mesoporous carbon catalysts in microwave heated reactor system.* Applied Catalysis B: Environmental, 2017. **219**: p. 173-182.
15. Chong, C.C., H.D. Setiabudi, and A.A. Jalil, *Dendritic fibrous SBA-15 supported nickel (Ni/DFSBA-15): A sustainable catalyst for hydrogen production.* International Journal of Hydrogen Energy, 2020. **45**(36): p. 18533-18548.

16. Al-Fatesh, A.S., et al., *Role of La_2O_3 as promoter and support in Ni/γ-Al_2O_3 catalysts for dry reforming of methane.* Chinese Journal of Chemical Engineering, 2014. **22**(1): p. 28-37.
17. Khoja, A.H., et al., *Thermal dry reforming of methane over La_2O_3 co-supported Ni/$MgAl_2O_4$ catalyst for hydrogen-rich syngas production.* RESEARCH ON CHEMICAL INTERMEDIATES, 2020.
18. Chein, R., et al., *Thermodynamic analysis of dry reforming of CH_4 with CO_2 at high pressures.* Journal of Natural Gas Science and Engineering, 2015. **26**: p. 617-629.
19. Baamran, K.S. and M. Tahir, *Ni-embedded TiO_2-$ZnTiO_3$ reducible perovskite composite with synergistic effect of metal/support towards enhanced H_2 production via phenol steam reforming.* Energy Conversion and Management, 2019. **200**: p. 112064.
20. Zhang, J., H. Wang, and A.K. Dalai, *Effects of metal content on activity and stability of Ni-Co bimetallic catalysts for CO_2 reforming of CH_4.* Applied Catalysis A: General, 2008. **339**(2): p. 121-129.
21. Seo, H.O., *Recent scientific progress on developing supported Ni catalysts for dry (CO_2) reforming of methane.* Catalysts, 2018. **8**(3): p. 110.
22. Domínguez, A., et al., *Biogas to syngas by microwave-assisted dry reforming in the presence of char.* Energy & fuels, 2007. **21**(4): p. 2066-2071.
23. Ruckenstein, E. and H. Wang, *Carbon deposition and catalytic deactivation during CO_2 reforming of CH_4 over Co/γ-Al_2O_3 catalysts.* Journal of Catalysis, 2002. **205**(2): p. 289-293.
24. Budiman, A.W., et al., *Dry reforming of methane over cobalt catalysts: a literature review of catalyst development.* Catalysis Surveys from Asia, 2012. **16**(4): p. 183-197.
25. Fan, M.S., A.Z. Abdullah, and S. Bhatia, *Catalytic technology for carbon dioxide reforming of methane to synthesis gas.* ChemCatChem, 2009. **1**(2): p. 192-208.
26. Topalidis, A., et al., *A kinetic study of methane and carbon dioxide interconversion over 0.5% Pt/$SrTiO_3$ catalysts.* Catalysis today, 2007. **127**(1-4): p. 238-245.

CHAPTER 5: CONCLUSIONS AND FUTURE PERSPECTIVES

5.1 Conclusions

This thesis focuses on the DRM process keeping in mind the basic theme of greenhousegases utilzation effectively with the catalsyt preparation and the comprehensive analysis of the catalytic activity and the catalyst deactivation induced by the reaction conditions. The carbon deposition resulting in catalyst deactivation is the major setback of the DRM reaction.

This study investigates the catalytic performance and stability of the prepared mixed TiO_2-$MgAl_2O_4$ supports over cobalt with different cobalt loading effect in the DRM reaction occurred in the fixed bed reactor. $MgAl_2O_4$ being acidic-basic support and TiO_2 support with anti-coking properties were prepared by hydrothermal method and both impregnated over cobalt with different loadings to make suitable combinations of composite.

Off the individual supports, metal-support combinations and composite tested for DRM activity, the composite Co/TiO_2-$MgAl_2O_4$ has shown the maximum values of X_{CH4} (72%) and X_{CO2} (80%) with higher selectivity and yield of H_2 and CO. With different cobalt loading effect over DRM, 5% Co/TiO_2-$MgAl_2O_4$ has shown the superior catalytic performance with higher activity and high stability of 75hrs. The maximum conversions, selectivity and yield results associated with 7.5% Co/TiO_2-$MgAl_2O_4$ are only for short TOS effect as long term usage brings instability because of carbon deposition leading to deactivation.

5% Co/TiO_2-$MgAl_2O_4$ has shown the average H_2/CO ratio of 0.9 for DRM up to 75 h stability test. $CoTiO_3$ reaction with carbon and the fast dissociation rate of CO_2 are the potential reasons of the higher CO production and syngas ratio below unity. The good activity and stability results of Co/TiO_2-$MgAl_2O_4$ suggests usage of the catalyst with

required modification in preparation for syngas production by DRM reaction on industrial scale.

5.2 Recommendations

DRM process finds promising future in the effective utilization of GHGs for syngas production. The major challenges in the DRM process are the development of the catalysts that are more resistant to deactivation and this need the usage of modern and highly developed advanced catalyst preparation methods. Also the reactor designs need to be developed with suitable reaction conditions for DRM processes. Moreover efforts should be done in order to optimize the design of catalyst to make the DRM process commercially viable

APPENDIX-PUBLICATIONS

A-1 Arslan Mazhar, Asif Hussain Khoja, Abul Kalam Azad, Faisal Mushtaq, Salman Raza Naqvi, Sehar Shakir, Muhammad Hassan, Rabia Liaquat and Mustafa Anwar. "*Performance analysis TiO_2 modified $Co/MgAl_2O_4$ catalyst for dry reforming of methane in a fixed bed reactor*." Energies (2021). (IF=2.7, Q2)

energies

MDPI

Type of the Paper (Article)

Performance analysis TiO_2 modified $Co/MgAl_2O_4$ catalyst for dry reforming of methane in a fixed bed reactor

Arslan Mazhar[1], Asif Hussain Khoja[1*], Abul Kalam Azad[2*], Faisal Mushtaq[3], Salman Raza Naqvi[4], Sehar Shakir[5], Muhammad Hassan[5], Rabia Liaquat[5], Mustafa Anwar[5]

[1] 1 Fossil Fuels Laboratory, Department of Thermal Energy Engineering, U.S.-Pakistan Centre for Advanced Studies in Energy (USPCAS-E), Na-tional University of Sciences & Technology (NUST), Sector H-12 Islamabad (44000), Pakistan. arslanmazhar32@gmail.com , astf@uspcase.nust.edu.pk
2 School of Engineering and Technology, Central Queensland University, 120 Spencer Street, Melbourne, VIC 3000, Australia. Email: a.k.azad@cqu.edu.au
3 Department of Chemical Engineering, Faculty of Engineering & Architecture, Balochistan University of Information Technology, Engineering and Management Sciences, Airport Road, Baleli, Quetta, Balochistan, Pakistan. faisalqta1977@gmail.com
4 School of Chemical and Materials Engineering (SCME), National University of Sciences & Technology (NUST), Sector H-12 Islamabad (44000), Pakistan. salman.raza@scme.nust.edu.pk
5 Department of Energy Systems Engineering, U.S.-Pakistan Centre for Advanced Studies in Energy (USPCAS-E), Na-tional University of Sciences & Technology (NUST), Sector H-12 Islamabad (44000), Pakistan. sehar@uspcase.nust.edu.pk , hassan@uspcase.nust.edu.pk , mustafa@uspcase.nust.edu.pk
* Correspondence: astf@uspcase.nust.edu.pk (A.H.K.); a.k.azad@cqu.edu.au (A.K.A)

Abstract: Co/TiO_2-$MgAl_2O_4$ has been investigated in a fixed bed reactor for dry reforming of methane (DRM) process. Co/TiO_2-$MgAl_2O_4$ is prepared by modified co-precipitation followed by the hydrothermal method. The prepared catalyst has been characterized by XRD, SEM, TGA and FTIR. The performance of Co/TiO_2-$MgAl_2O_4$ for the dry reforming of methane (DRM) process is investigated at reactor with a temperature of 850 °C, feed ratio (CO_2/CH_4) =1, catalyst loading 0.5g and the feed flow rate of 20 mL min^{-1}. The effect of supports individually, interaction with metal and in the composite has been studied for the catalytic activity with the composite showing significantly improved results. Moreover, among the Co loadings studied, 5%Co over TiO_2-$MgAl_2O_4$ composite demonstrated better catalytic performance. The 5%Co/TiO_2-$MgAl_2O_4$ improves the CH_4 and CO_2 conversion up to 70% and 80%, respectively, while the selectivity of H_2 and CO improves to 43% and 46.5%, respectively. The syngas ratio of 0.9 is due to the excess amount of CO produced because of the higher conversion rate of CO_2 and surface carbon reaction with oxygen species. Furthermore, in time on stream (TOS) test, the catalyst exhibits 75 hours of stability with significant catalytic activity. The catalyst's potential lies in catalyst stability and catalytic performance results while encouraging further investigation and use of the catalyst for the long run DRM process.

Citation: Lastname, F.; Lastname, F.; Lastname, F. Title. *Energies* 2021, 14, x. https://doi.org/10.3390/xxxxx

Academic Editor: Firstname Lastname

Received: date
Accepted: date
Published: date

A2 Asif Hussain Khoja, Mustafa Anwar, Sehar Shakir, Muhammad Taqi Mehran, Arslan Mazhar, Adeel Javed, and Nor Aishah Saidina Amin. "*Thermal dry reforming of methane over La_2O_3 co-supported Ni/$MgAl_2O_4$ catalyst for hydrogen-rich syngas production*." Research on Chemical Intermediates 46 (2020): 3817-3833. (IF=2.62, Q2)

Research on Chemical Intermediates (2020) 46:3817–3833
https://doi.org/10.1007/s11164-020-04174-z

Thermal dry reforming of methane over La_2O_3 co-supported Ni/$MgAl_2O_4$ catalyst for hydrogen-rich syngas production

Asif Hussain Khoja[1] · Mustafa Anwar[1] · Sehar Shakir[1] · Muhammad Taqi Mehran[2] · Arslan Mazhar[1] · Adeel Javed[1] · Nor Aishah Saidina Amin[3]

Received: 27 March 2020 / Accepted: 6 May 2020 / Published online: 22 May 2020

Abstract
The excess emission of greenhouse gases (GHGs) such as CO_2 and CH_4 is posing an acute threat to the environment, and efficient ways are being sought to utilize GHGs to produce syngas (H_2, CO) and lighter hydrocarbons (HCs). In this study, the dry reforming of methane (DRM) has been carried out at 700 °C using La_2O_3 co-supported Ni/$MgAl_2O_4$ nano-catalyst in a fixed bed thermal reactor. The catalyst is characterized using various techniques such as XRD, FESEM, EDX-mapping, CO_2-TPD, H_2-TPR and TGA. The modified $MgAl_2O_4$ shows the flake type structure after the addition of La_2O_3. The TPR and TPD analysis shows the highly dispersed metal and strong basic nature of the catalyst consequently enhances the conversion of CO_2 and CH_4. The highest conversion for CH_4 is 87.3% while CO_2 conversion is nearly 89.5% in 20 h of operation time. The selectivity of H_2 and CO approached 50% making the H_2/CO ratio above unity. In the longer time-on-stream (TOS) test, the catalyst shows elevated potential for longer runs showcasing better catalytic activity. The stability of the catalyst is indicated via a proposed reaction mechanism for DRM in operating conditions. Moreover, TGA indicates the lower weight loss of spent catalyst which ascribed the lower formation of carbon during TOS 20 h.

Keywords Dry reforming of methane · thermal reactor · $MgAl_2O_4$ · H_2 production · syngas

A3 Asif Hussain Khoja, Arslan Mazhar, Faisal Saleem, Muhammad Taqi Mehran, Salman Raza Naqvi, Mustafa Anwar, Sehar Shakir, Nor Aishah Saidina Amin, and Muhammad Bilal Sajid. "*Recent developments in catalyst synthesis using DBD plasma for reforming applications*." International Journal of Hydrogen Energy (2021). (IF=5.95, Q1)

INTERNATIONAL JOURNAL OF HYDROGEN ENERGY 46 (2021) 15367–15388

Available online at www.sciencedirect.com

ScienceDirect

journal homepage: www.elsevier.com/locate/he

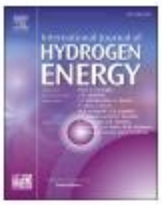

Review Article

Recent developments in catalyst synthesis using DBD plasma for reforming applications

Asif Hussain Khoja [a,*], *Arslan Mazhar* [a], *Faisal Saleem* [b], *Muhammad Taqi Mehran* [c], *Salman Raza Naqvi* [c], *Mustafa Anwar* [d], *Sehar Shakir* [d], *Nor Aishah Saidina Amin* [e], *Muhammad Bilal Sajid* [a]

[a] *Fossil Fuel Laboratory, Department of Thermal Energy Engineering, U.S-Pakistan Centre for Advanced Studies in Energy (USPCASE), National University of Sciences & Technology (NUST), H-12 Sector, 44000, Islamabad, Pakistan*
[b] *Department of Chemical and Polymer Engineering, University of Engineering and Technology, Faisalabad Campus, Lahore, Pakistan*
[c] *School of Chemical & Materials Engineering (SCME), National University of Sciences & Technology (NUST), H-12 Sector, 44000, Islamabad, Pakistan*
[d] *Department of Energy Systems Engineering, U.S-Pakistan Centre for Advanced Studies in Energy (USPCASE), National University of Sciences & Technology (NUST), H-12 Sector, 44000, Islamabad, Pakistan*
[e] *Chemical Reaction Engineering Group (CREG), Faculty of Chemical and Natural Resources Engineering, Universiti Teknologi Malaysia, 81310, UTM Skudai, Johor, Malaysia*

HIGHLIGHTS

- The NTP plasma techniques for catalyst synthesis is overviewed.
- The DBD plasma-treated catalyst is summarised.
- Prospects of DBD for catalyst synthesis in H_2/syngas production is presented.

GRAPHICAL ABSTRACT

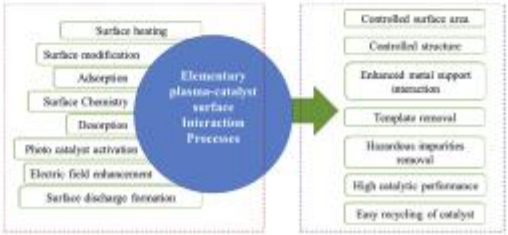

ARTICLE INFO

ABSTRACT